

Time and space variations of the O₂/N₂ ratio observed over the western North Pacific using a cargo aircraft C-130H

Shigeyuki Ishidoya^{1*}, Kazuhiro Tsuboi², Hidekazu Matsueda², Shohei Murayama¹, Yousuke Sawa², Yosuke Niwa², Shoichi Taguchi¹, Masamichi Nakamura³, Taro Kawasato³, Kazuyuki Saito³, Shinya Takatsuji³, Kentaro Tsuji³, Hidehiro Nishi³, Koshiro Dehara³, Yusuke Baba³

¹AIST, ²Meteorological Research Institute, ³Japan Meteorological Agency

The atmospheric O₂/N₂ ratio ($d(O_2/N_2)$) has been observed at many ground-based stations since the early 1990s to elucidate the global CO₂ budget (e.g. Manning and Keeling, 2006), however, airborne observations of $d(O_2/N_2)$ in the free troposphere are very limited (e.g. Ishidoya et al., 2012). In this study, the air samples collected using a cargo aircraft C-130H in service between Atsugi Base (35.45 N, 139.45 E) and Minamitorishima (MNM; 24.28 N, 153.98 E) have been analyzed for $d(O_2/N_2)$, Ar/N₂ ratio ($d(Ar/N_2)$), $d^{15}N$ of N₂, $d^{18}O$ of O₂ and $d^{40}Ar$ to clarify time and space variations of the $d(O_2/N_2)$ in the mid-troposphere.

The observations onboard the C-130H are conducted once per month, and 24 air samples are collected into 1.7 L Titanium flasks during the level flight at an altitude about 6 km and descent toward MNM (Tsuboi et al., 2012). 6 air samples are also collected into the similar flasks at the ground surface in MNM around the same time period with the C-130 H observation. The total of 30 air samples are analyzed for CO₂, CH₄, N₂O and CO concentration at Japan Meteorological Agency, then analyzed for $d(O_2/N_2)$, $d(Ar/N_2)$, $d^{15}N$ of N₂, $d^{18}O$ of O₂ and $d^{40}Ar$ at AIST since May 2012.

The $d^{15}N$ of N₂, $d^{18}O$ of O₂ and $d^{40}Ar$ are known to be almost constant in the troposphere, and the $d(Ar/N_2)$ shows slight seasonal cycle at the ground surface with the peak-to-peak amplitude of 10-30 per meg (e.g. Casser et al., 2008). However, the $d(Ar/N_2)$, $d^{15}N$ of N₂, $d^{18}O$ of O₂ and $d^{40}Ar$ from the C-130H observations were found to be significantly different from the surface values at MNM. Especially, the $d(Ar/N_2)$ of the air samples collected during the level flight were higher by about 800 per meg than the surface values. Such the large variations in the $d(Ar/N_2)$ were considered to be due to some sort of the artificial fractionations of Ar and N₂. Therefore, we examined the relationships between $d(Ar/N_2)$, $d^{18}O$ of O₂ and $d^{40}Ar$ and $d^{15}N$ of N₂ to clarify the cause of the fractionation. The obtained relationships were highly consistent with those expected from the fractionation due to the thermal diffusion (Ishidoya et al., 2013), which would be attributed to the branching of flow paths (e.g. Bender et al., 2005) of the ambient air supplied from the jet engine to pressurize the cabin of the C-130H. Taking these facts into consideration, we corrected the $d(O_2/N_2)$ obtained from the C-130H observation for the fractionation by using an experimentally-determined relationship of the $d(Ar/N_2)/d(O_2/N_2)$ due to the thermal diffusion and the measured values of the $d(Ar/N_2)$. Because the $d(Ar/N_2)/d(O_2/N_2)$ ratio due to the thermal diffusion and the measurement precision of the $d(Ar/N_2)$ were about 4.5 and +5 per meg, respectively, the uncertainty of $d(O_2/N_2)$ associated with the correction was estimated to be about +1 per meg. This uncertainty is smaller enough than +4.8 per meg (+1 ppm) of the precision required for the precise observation of the atmospheric $d(O_2/N_2)$. Therefore, it is suggested that variations of the $d(O_2/N_2)$ in the free troposphere are observable using the C-130H by applying the correction method.

The corrected $d(O_2/N_2)$ and CO₂ concentration varied seasonally almost in opposite phase at all heights. The average Atmospheric Potential Oxygen (APO = O₂ + 1.1 x CO₂) (Stephens et al., 1998) during the observation period (May - December 2012) decreased with increasing altitude, which implied the net O₂ outgassing from the ocean around MNM for the period. In the presentation, we will also discuss the characteristic variations of the $d(O_2/N_2)$ observed in the free troposphere based on the analyzed results of comparisons of the $d(O_2/N_2)$ with the CO₂, CH₄, N₂O and CO concentration as well as the backward trajectories for the observation dates. The correction method employed in this study will make it possible to observe the $d(O_2/N_2)$ precisely using air samples collected without special sampling techniques to reduce the fractionations of the molecules.

Keywords: aircraft observation, atmospheric O₂/N₂ ratio, Atmospheric Potential Oxygen (APO), correction method for fractionation of O₂ and N₂

Analyses for CO₂ source in the urban area: measurement of stable isotope ratio of CO₂ and CO₂, CO, NO_x

Akie Yuba^{1*}, Kenshi Takahashi², Tomoki Nakayama¹, Yutaka Matsumi¹

¹Nagoya University, Solar-terrestrial environmental laboratory, ²Kyoto University, Research institute for sustainable humanosphere

CO₂ has the most effect on the global climate change because CO₂ has the largest positive radiative forcing (IPCC 2007). The accurate estimation of the CO₂ emission and loss flux are necessary to improve the prediction of the global climate change in the future, because the variations of CO₂ concentration substantially contributes to the variations of the global radiative forcing. CO₂ concentration varies due to the emission from the gasoline and natural gas combustion, biomass burning, and ecosystem respiration, the absorption due to the photosynthesis, the absorption into ocean and emission from the ocean surface. In the urban area, the variation of CO₂ concentration depends on the anthropogenic emission such as the fossil fuel combustion (gasoline and natural gas) and background CO₂ concentration mainly.

We conducted the continuous measurement of carbon and oxygen isotope ratios of CO₂ ($\delta^{13}\text{C}$, $\delta^{18}\text{O}$) using the infrared absorption laser spectrometer. The infrared absorption laser spectrometer can continuously measure $\delta^{13}\text{C}$, $\delta^{18}\text{O}$ in high time resolution (10 seconds). The measurement period was from July 20 to August 10, 2012 at Nagoya University. Simultaneously, we measured the concentrations of nitrogen oxides, CO, water vapor and stable isotope ratios of water vapor (δD and $\delta^{18}\text{O}$). The variations of CO₂ concentrations, $\delta^{13}\text{C}$ and $\delta^{18}\text{O}$ shows the contribution of the fossil fuel combustion and ecosystem respiration to the carbon cycle in the urban area.

Measured CO₂ concentrations and stable isotope ratios ($\delta^{13}\text{C}$, $\delta^{18}\text{O}$) show the diurnal variation in the measurement period. CO₂ concentrations decreased in the daytime and had a peak in the nighttime. On the other hand, $\delta^{13}\text{C}$ and $\delta^{18}\text{O}$ had a peak in the daytime and decreased in the nighttime. This indicates that the variations of CO₂ concentration were substantially affected by the ecosystem respiration and photosynthesis in the urban area. We conducted the keeling plot analyses for $\delta^{13}\text{C}$ and $\delta^{18}\text{O}$ in the nighttime to estimate the contributions of the fossil fuel combustion, biomass burning, and ecosystem respiration. In addition of the keeling plot analyses, we estimated CO₂ source from the relationship between the variations of CO and CO₂ concentrations. CO is emitted by the fossil fuel combustion and biomass burning mainly, while, CO₂ generated by the fossil fuel combustion, biomass burning and ecosystem respiration. Therefore, the relationship between CO and CO₂ concentration shows CO₂ source; the larger ratios of CO to increment of CO₂ from the background level (δCO_2) shows the contribution of the fossil fuel combustion or biomass burning, on the other hand, the smaller ratios of CO to δCO_2 shows the contribution of the ecosystem respiration. We will discuss the source of CO₂ from the analyses of the ratios of CO to δCO_2 and keeling plot.

Keywords: Carbon dioxide, Stable isotope ratio, Laser spectrometry, CO₂ Source estimation, Carbon monoxide

NO₂ observed by MAX-DOAS at Fukue Island: Comparison to ground-based observations and long-term variations

Yugo Kanaya^{1*}, Hitoshi Irie², Hisahiro Takashima³, Fumikazu Taketani¹, Yuichi Komazaki¹, Xiaole Pan¹, Hiroshi Tanimoto⁴, Satoshi Inomata⁴, Tomoki Nakayama⁵, Yutaka Matsumi⁵

¹RIGC/JAMSTEC, ²Chiba University, ³Fukuoka University, ⁴NIES, ⁵Nagoya University

Since spring 2009, we conduct observations of NO₂ and aerosols at Fukue Island (32.75N, 128.68E) using MAX-DOAS (Multi-Axis Differential Optical Absorption Spectroscopy), in addition to surface monitoring of O₃, PM_{2.5} and black carbon, to elucidate regional air pollution over East Asia. Differential slant column densities (DSCDs) of NO₂ and O₄ are first determined for the UV/vis spectra observed at low elevation angles (3, 5, 10, 20, and 30 degrees) with respect to the zenith observations used as reference. Aerosol profile is first retrieved such that the O₄ DSCDs are consistent with radiative transfer and then the tropospheric column density of NO₂ and its vertical profile are optimally estimated. At Fukue Island, in-situ NO₂ observations were made using a chemiluminescence instrument equipped with a photolytic converter in May-June 2009 and a laser-induced fluorescence instrument in March-June 2010, respectively. These data were successfully used to evaluate the NO₂ quantities derived from MAX-DOAS observations. We analyzed diurnal to seasonal variations of NO₂ in 2009-2012, derived from MAX-DOAS. Wintertime maxima were regularly observed during this period. High NO₂ concentrations were recorded when air mass was rapidly transported from Korean Peninsula. Such transport was sometimes evident in spring period, affecting the ozone production regime there.

Keywords: Nitrogen Oxides, MAX-DOAS, instrument comparison, long-term variation, aerosol

An evaluation of the CMAQ reproducibility of satellite tropospheric NO₂ data at different local times over East Asia

Hitoshi Irie^{1*}, Kazuyo Yamaji², Kohei Ikeda², Itsushi Uno³, Syuichi Itahashi³, Toshimasa Ohara⁴, Jun-ichi Kurokawa⁵

¹Chiba University, ²JAMSTEC, ³Kyusyu University, ⁴NIES, ⁵ACAP

Despite the importance of the role of nitrogen dioxide (NO₂) in the troposphere, causes leading to a discrepancy between satellite-derived and modeled tropospheric NO₂ vertical column densities (VCDs) over East Asia remain unclear. Here the reproducibility of satellite tropospheric NO₂ VCD data by a regional atmospheric chemistry model (CMAQ) with the Regional Emission inventory in ASia (REAS) Version 2 is evaluated from the viewpoint of the diurnal variation of tropospheric NO₂ VCDs, where satellite observations at different local times (SCIAMACHY/ENVISAT, OMI/Aura, and GOME-2/Metop-A) are utilized considering literature validation results. As a case study, we concentrate on June and December 2007 for a detailed evaluation based on various sensitivity runs, for example with different spatial resolutions (80, 40, 20, and 10 km) for CMAQ. For June, CMAQ generally reproduces absolute values of satellite NO₂ VCDs and their diurnal variations over all selected 12 diagnostic regions in East Asia. In contrast, a difficulty arises in interpreting a significant disagreement between satellite and CMAQ values over most of the diagnostic regions in December. The disagreement cannot be explained by any sensitivity runs performed in this study. To address this, more investigations, including further efforts for satellite validations in wintertime, are needed.

Keywords: NO₂, CMAQ, satellite data, diurnal variation

Multiple species constraints on surface NO_x emission inversion

Kazuyuki Miyazaki^{1*}, Henk Eskes²

¹Japan Agency for Marine-Earth Science and Technology, ²Royal Netherlands Meteorological Institute (KNMI)

Satellite NO₂, CO, O₃, and HNO₃ data are assimilated into a chemical transport model to estimate global surface NO_x emissions and their seasonal variation in 2007. The data assimilation of data for multiple species provides comprehensive constraints on the NO_x emissions by limiting model errors in NO_x chemistry. The non-NO₂ data changed the regional and hemispheric monthly total NO_x emissions by 50% and 13-29%, respectively. These large changes introduced by the inclusion of non-NO₂ data imply a large uncertainty in the NO_x emissions inverted from NO₂ data only. Compared to the emission inventories, the estimated NO_x emissions show enhanced seasonal variations with the maximum emissions at most of the northern mid-latitudes occurring 1-2 months earlier. An analysis of the background error covariance demonstrates that additional constraints from other chemically related species (e.g., isopren and formaldehyde) have the potential to further improve surface NO_x emission analyses.

Keywords: NO_x emission, Data assimilation, Satellite observation

Trend and interannual variation of the stratospheric CO₂ in the past 25 years

Satoshi Sugawara^{1*}, Shuji Aoki², Takakiyo Nakazawa², Shigeyuki Ishidoya³, Shinji Morimoto⁴, Sakae Toyoda⁵, Hideyuki Honda⁶

¹Miyagi Univ. of Education, ²CAOS, Tohoku Univ., ³AIST, ⁴NIPR, ⁵Tokyo Institute of Technology, ⁶ISAS/JAXA

Systematic collections of stratospheric air samples have been carried out over Japan since 1985, using a balloon-borne cryogenic sampler. The stratospheric air samples have been collected almost once a year or two years at 11 assigned heights, ranging from the tropopause to 30 - 35 km. The air samples were analyzed for various gas concentrations, such as CO₂, CH₄, N₂O, and SF₆, and their isotopes. Measurements of the stratospheric CO₂ concentration are one of the most promising methods to detect possible changes in the stratospheric circulation, because chemical loss and production are negligible in the stratosphere and its long-term trend in the troposphere is propagated into the stratosphere, with some time lag. Increasing trend of the CO₂ concentration was clearly found at heights above 20-25 km, where the CO₂ concentration becomes almost constant vertically. To clarify the difference of the secular CO₂ increases between the mid-stratosphere and the troposphere, the average values of the CO₂ concentration, calculated from the balloon data obtained at heights above 20-25 km, were compared with annual mean CO₂ concentrations at Mauna Loa (MLO) observed by NOAA/ESRL. The average increase rate of the CO₂ concentration in the mid-stratosphere, calculated by using a least-squares method, was 1.55(+0.03) ppmv/year. This value is significantly smaller than 1.73(+0.03) ppmv/year calculated for the same period for MLO data. Considering that the mid-stratospheric CO₂ concentration corresponds to the tropospheric values earlier by 4-5 years, the CO₂ increase rate in the stratosphere should be compared with the tropospheric values shifted by the same years. The average increase rate, thus calculated for the period 1981-2005, was 1.62(+0.03) for MLO data. This value is slightly smaller than those described above, due to interannual variations of CO₂ increase rate in the troposphere, but still larger than the stratospheric value. These facts imply that the concentration difference between the troposphere and mid-stratosphere gradually increased during the last 25 years. The interannual CO₂ variation in the mid-stratosphere was first discovered by our balloon measurements. The secular CO₂ increase in the mid-stratosphere is not monotonous, probably due to the propagation of interannual variations in tropospheric CO₂, being accompanied by time delay. The CO₂ anomalies in the mid-stratosphere, calculated as deviations from the second order polynomial trend and then shifted by -4.5 years, are fairly correlated with those in the troposphere. Such a correlation is found especially in CO₂ anomalies observed in the troposphere for a few years after 1991, which is known as the Pinatubo anomaly. This result suggests that the stratospheric air age can be newly estimated from the phase shift of the interannual CO₂ variations.

Keywords: CO₂, Stratosphere, Long-term trend

Relationship between polar stratospheric cloud types and ozone destruction

Masanori Takeda^{1*}, Hideaki Nakajima², Hiroshi Tanaka³

¹Graduate School of Life and Environmental Sciences, University of Tsukuba, ²National Institute for Environmental Studies, ³Center for Computational Sciences, University of Tsukuba

Polar stratospheric clouds (PSCs) can appear at a temperature lower than nitric acid trihydrate (NAT) saturation temperature in the polar lower stratosphere. PSCs cause large ozone destruction by heterogeneous reactions on particle surface and denitrification by gravitational sedimentation in the polar spring. PSCs can be classified into three major types (Type Ia, Ib, and II). Type Ia is a solid particle which is comprised of NAT. Type Ib is a liquid particle called supercooled ternary solution (STS) which is composed of HNO₃, H₂SO₄, and H₂O. Type II is water ice particle.

In general, the probability of PSC formation is closely related to the magnitude of chemical ozone loss. However, Terao et al. (2012) showed that the average ozone destruction rate in 1996 and 2000 Arctic winter were different when the average PSC sighting probabilities were similar. As one of the possible reason, we assumed a hypothesis that PSC types may influence the magnitude of ozone destruction. Therefore, we investigated the relationship between PSC types and the ozone destruction rate statistically.

We used the observational data from CALIOP lidar on board the satellite CALIPSO. PSCs observed by CALIOP were categorized into 6 types; i.e. Mix 1, Mix 2, Mix 2-enhanced, Ice, Wave-ice, and STS (Pitts et al. 2007, 2009, 2011). Mix is a PSC type category which contains NAT and STS. We quantified the ozone destruction rate of PSC types observed in 2007 Antarctic winter and in 2009/10 Arctic winter by using a Satellite-Match technique with the observational data of MLS on board the satellite Aura. As a result, it was confirmed that the average ozone destruction rate were different in every PSC type. Especially, the average ozone destruction rate of STS and Mix were larger.

Furthermore, we investigated the relationship between backscatter ratio as an index of particle number density and ozone destruction rate for every PSC type. As a result, it was confirmed that there are positive correlation between backscatter ratio and ozone destruction rate in all PSC types. As a result of the simple linear regression fitting using backscatter ratio as an independent variable, the regression coefficient for Mix PSC is the largest. It is thought that PSCs including NAT and STS have the highest potential for large-scale ozone destruction.

Keywords: Polar stratospheric cloud, Ozone destruction, Satellite-Match technique, CALIPSO

Unusual aerosol enhancement in Antarctic troposphere during spring

Keiichiro Hara^{1*}, Masahiko Hayashi¹, Masanori Yabuki², Masataka Shiobara³

¹Fukuoka Univ., ²Kyoto Univ. RISH, ³NIPR

Antarctic region is isolated from the other continents with human activities. Nevertheless, high aerosol concentrations (Antarctic haze) were observed occasionally near surface at Syowa Station, Antarctica, during winter ? spring (Hara et al., JGR, 2010). Vertical distributions of the Antarctic haze were obtained in a few tethered-balloon-borne aerosol measurements and a lunched-balloon borne aerosol measurement at Syowa Station (Hara et al., ACP, 2011). Spatial features of the aerosol enhancement, however, have not been discussed well. This study aims to elucidate spatial features of aerosol enhancement (Antarctic haze) over Syowa Station by simultaneous measurements in near surface ~ upper atmosphere. Condensation particle counter (CPC), optical particle counter (OPC), and aethalometer were used to measure physical properties of aerosols near surface. Micro-pulse LIDAR (MPL) and aerosol sonde (balloon-borne OPC) were used to measure vertical distributions of aerosol particles over Syowa Station in this study. Balloon-borne aerosol measurements carried out under aerosol enhanced conditions near surface on 14 August and 6 September, 2012. High aerosol enhanced conditions near surface on 13-16 August, 2012 were observed immediately after storm condition. MPL measurements exhibited that aerosols were enhanced in ~ ca. 2.5 km on 13 - 16 August. In contrast, aerosol enhancement near surface on 5 - 7 September, 2012 appeared suddenly under the calm wind conditions. Although aerosol number concentrations near surface dropped markedly before the aerosol enhancement (00-15UT on 5 September), strong aerosol enhancement was found around 1-1.5 km since 05UT on 5 September in the MPL measurements. Although strong aerosol enhanced layer was distributed mostly in ~3km, high relative backscatter was observed occasionally in 3 ~ 4 km on 6 September. Here, we discuss aerosol features and distributions in the twice simultaneous measurements.

Identification of Sources of Lead in the Atmosphere by its Speciation and Isotopic Composition

Kohei Sakata^{1*}, Aya Sakaguchi¹, Masaharu Tanimizu², Yuichi Takaku³, Yoshio Takahashi¹

¹Department of Earth and Planetary Systems Science, Hiroshima University, ²Kochi Institute, Japan Agency for Marine-Earth Science and Technology, ³Institute for Environment Sciences

1. Introduction

Recently, chemical reactions of major elements occurred in the atmosphere have been clarified, whereas those of trace metals have not. In particular, formation processes of Pb species, which is concerned to cause a health hazard, are still unclear. The identification of species and formation process of Pb is important to evaluate the human hazards. In addition, Pb species is expected to be used as a transboundary pollution tracer, because Pb species are different depending on each emission area. In this study, Pb species in size-fractionated aerosol sample were determined by XAFS spectroscopy together with the Pb isotope ratios to identify the formation mechanisms of Pb species in aerosol.

2. Sampling and Analysis Methods

Size-fractionated aerosol samples were collected by a high-volume cascade impactor in Higashi-Hiroshima. Sampling period was from 9th Oct. 2012 to 23th Oct. 2012 (2 weeks). Candidates of Pb source in atmosphere, fly ash of municipal solid incinerator (MSWI), heavy oil combustion, road dust and resuspension particles on the roof, were also collected. Weathered Hiroshima-granite, which is crustal material of the sampling area, was also collected as a possible natural Pb source. Lead species were determined by X-ray absorption fine structure (XAFS) spectroscopy. Heavy metals concentrations were measured by ICP-MS. Lead isotope ratios were determined by MC-ICP-MS with Tl doping technique after appropriate treatments.

3. Results and Discussion

Lead species were different between coarse and fine aerosol particles. Lead species in coarse aerosol particles were PbC_2O_4 , $2\text{PbCO}_3\text{-Pb(OH)}_2$, and $\text{Pb(NO}_3)_2$. Lead sources of coarse aerosol particles can be road dust because main Pb components in road dust were PbC_2O_4 and $2\text{PbCO}_3\text{-Pb(OH)}_2$. This result was also suggested by EFs of Cu and Sb which are good indicators of road dust. Lead nitrate in coarse aerosol, which was not contained in road dust, might be formed by chemical reaction of natural Pb with gas-phase HNO_3 in the atmosphere. In contrast, Pb species of fine aerosol particles were PbC_2O_4 , PbSO_4 , and $\text{Pb(NO}_3)_2$. Major Pb sources in fine aerosol particles are fly ash of MSWI and heavy oil combustion based on the determination of Pb species in these materials examined in this study. This result was also supported by size-distributions of Cd, Ni and V.

In our presentation, the results of Pb isotopic composition will be discussed together with Pb species in aerosol samples.

Keywords: Aerosol, Lead species, Lead isotope, XAFS spectroscopy, MC-ICP-MS

Behavior of Heavy Metal-containing PM_{2.5} Transported from the Asian Continent :Single-particle MS and Chemical Analysis

Takehiro Hidemori^{1*}, Tomoki Nakayama¹, Yutaka Matsumi¹, Akihiro Yabushita², Masafumi Ohashi³, Naoki Kaneyasu⁴, SATOSHI IREI⁵, Akinori Takami⁵, Ayako Yoshino⁶, Ryota Suzuki⁶, Yayoi Yumoto⁶, Shiro Hatakeyama⁶

¹STE Lab, Nagoya Univ, ²Kyoto Univ, ³Kagoshima Univ, ⁴NIES, ⁵AIST, ⁶TUAT

The Asian continent is an important source region of atmospheric aerosols with different origins and metals including combustion, dust storms and industrial and residential emissions. Some studies were reported polluted aerosols are transported from the Asian continent over from winter to spring by the outflow of the Asian air masses. In order to better understand characteristics of these aerosols, we investigated the chemical characteristics of individual aerosol particles by using a laser ionization single-particle mass spectrometer (LISPA-MS) along with other aerosol and gas measurements in the spring and winter of 2010 in Fukue Island, Nagasaki. Trace gas concentrations, total mass concentration of atmospheric aerosols (TEOM), mass concentrations of sulfate, nitrate, organics, and ammonium (AMS), and organics, trace metals (HVI2.5) were utilized to get quantitative information during the field campaign. We focused on the fine particle with lead (Pb) -containing aerosols as lead is considered a criteria air pollutant with wide range of health effects.

Over the measurement period, the LISPA-MS obtained ca. 90,000 (spring) and ca. 30,000 (winter) positive single-particle mass spectra. Pb-containing particles accounted for 2-4% of all the measured particles. Pb-containing aerosols were classified four major particle types from the obtained mass spectral patterns. The K-Fe-Zn type is characterized by the presence of an intense K ion peak with Fe, sodium Na, and zinc Zn and it makes up 40-60% of the total Pb-containing particles. The aerosol type with intense K, Fe, Zn without Al, Sn, and V is attributed coal combustion from the previous laboratory experiment. The Al-Ca type is characterized by the specific presence of aluminum (Al) ion peak and calcium (Ca). Since Al and Ca is a marker of mineral dust, the Al-Ca type is assigned dust aerosols. The V type is characterized the specific presence of vanadium ion peaks (V and VO) which is a marker of fuel oil combustion and refining. The Sn type is characterized by the specific presence of a tin (Sn) which is a marker of industrial waste incineration. While air mass reached to Fukue Island from China continent for back trajectory, the number of Pb-containing particles showed a significant increase. The temporal variation of Pb-containing particles except from V-type shows well-correlated with that of the fraction of dust particles which is SiO₃ containing particles analyzed from the negative mass spectra. In conclusion, the LISPA-MS measurements indicated that Pb-containing particles originated from the anthropogenic source such as coal combustion and industrial waste incineration accounted for 40-70% and were mainly transported from China continent.

Keywords: PM_{2.5}, long-range transport, single-particle laser ionization mass spectrometer, Heavy metal-containing aerosols

Solubility of iron in aerosols of volcanic origin with iron speciation analysis

Aya Miyahara^{1*}, Yoshio Takahashi¹, FURUTANI, Hiroshi², Mitsuo Uematsu²

¹Department of Earth and Planetary Systems Science, Graduate School of Science, Hiroshima University, ²Atmosphere and Ocean Research Institute, The University of Tokyo

In high nutrient low chlorophyll (HNLC) region, which covers 20% of the world oceans, growth of phytoplankton is limited by iron (Fe) concentration (Martin and Fitzwater, 1988). It has been suggested that aerosols can be an important supply source of Fe to the HNLC region. The solubility in ocean of Fe in aerosols, in turn, depends on its chemical species, but the Fe species in the aerosols have not been fully clarified. Therefore, the aim of this study is to determine the Fe chemical species and its solubility in aerosols of various sources. In particular, there have been few studies on the Fe speciation and solubility in aerosols of volcanic origin. Thus, marine aerosol samples of volcanic origin were examined in this study. The aerosol samples were collected from the Northwestern Pacific during research cruise of Hakuho-Maru (KH-08-2) in summer in 2008. As a result of backward trajectory analysis for the sample (Leg.1-5) when high sulfate concentration was detected, it was suggested that the aerosol samples was supplied from the Okmok volcano in the Aleutian Islands of Alaska as volcanic ashes. Hence, the volcanic ashes (< 20, 20-32, and 32-250 micron) of Okmok volcano received from Alaska Volcano Observatory were also studied as well as yellow dusts (CJ-1, CJ-2, and Gobi Kosa Dust) for comparison.

The Fe/Al ratio in the Leg.1-5 sample was identical to that of the volcanic ash sample, showing that the aerosols collected during the Leg.1-5 is supplied from the eruption of the Okmok volcano, which reinforces the suggestion by the backward trajectory analysis. Sulfur K-edge XANES showed that sulfide originally contained in the volcanic ash changed into sulfate possibly due to the alteration during the transport to the Northwestern Pacific. Iron K-edge XANES analysis showed Leg.1-5 contained ferrihydrite (60%), magnetite (28%), and iron(II) sulfate (12%), whereas volcanic ashes (< 20 micron) contained augite (57%), fayalite (25%), and pyrite (18%). CJ-1 and CJ-2 contained illite, ferrihydrite, and chlorite, while Gobi Kosa Dust contained illite, ferrihydrite, and hematite. In addition, the average valence of Fe determined by pre-edge fitting of Fe K-edge XANES showed that the ratio of ferric iron of Leg.1-5 (average valence of Fe = 2.4) is higher than that of volcanic ashes (average valence of Fe = 2.1). These results showed aerosols of volcanic origin released into the atmosphere were altered and oxidized while being transported.

The total Fe concentration (T-Fe) in samples after acid decomposition and the dissolved Fe concentration (D-Fe) in samples extracted by MQ water or simulated seawater (pH 8) were determined by ICP-AES. The Fe solubility (Fe_s) here was defined as the percentage of Fe released in the solution after 24 h: $Fe_s (\%) = (D-Fe/T-Fe) \times 100$. The results showed that the solubility to seawater (Fe_s -SW) of Fe contained in the aerosol samples of volcanic origin is larger than that of yellow dusts by a factor of more than 1000. Generally speaking, Fe solubility depends on the valence of Fe, that is, the solubility decrease with the increase in the ratio of ferric iron for ferrous iron. In this study, however, the Fe solubility of the aerosol samples is higher than that of volcanic ashes mainly due to the formation of iron(II) sulfate, highly soluble species, as shown in the XAFS spectra. This is why volcanic ashes which originally contained insoluble Fe changed into the aerosols with high soluble Fe content.

Although the average emission of fine volcanic ash (176-256 Tg/yr; Durant et al., 2010) into the atmosphere is less than that of annual terrigenous dust load (1000-3000 Tg/yr; Tegen and Schepanski, 2009) by a factor of 1/10, the soluble Fe content in the aerosols supplied as volcanic ashes cannot be underestimated due to the very high soluble Fe content in the aerosols of volcanic origin.

Keywords: Fe, speciation, solubility, aerosol, volcanic ash, dust

Molecular distributions of organic aerosols collected over the western North Atlantic

Kimitaka Kawamura^{1*}, Kaori Ono¹, Eri Tachibana¹, Trish Quinn²

¹Institute of Low Temperature Science, Hokkaido University, ²NOAA PMEL

Marine aerosols were collected over the western North Atlantic from Boston to Bermuda during the cruise of R/V Ronald H. Brown in August 2012 using a high volume air sampler and quartz fiber filter. Aerosol filter samples were analyzed for OC/EC, ions, dicarboxylic acids and various SOA tracers using carbon analyzer, ion chromatograph, GC/FID and GC/MS, respectively. Homologous series of low molecular weight dicarboxylic acids (C2-C12) were detected with a predominance of oxalic acid. Their concentrations decreased from the coastal region to the open ocean. Isoprene SOA tracers and monoterpene SOA tracers were also detected with the higher concentrations near the east coast of North America. Sugar compounds that are derived from pollen (sucrose and fructose) and fungal spores (arabitol, mannitol and trehalose) showed higher concentrations in the coastal region than the open ocean.

Keywords: marine aerosols, organic compounds, LMW dicarboxylic acids, SOA tracers, Biomass burning tracers, pollen and fungal spore tracers

Investigation on the SOA formation mechanism in isoprene ozonolysis by chemical ionization mass spectrometry

Satoshi Inomata^{1*}, HIROKAWA, Jun², Yosuke Sakamoto², Hiroshi Tanimoto¹, Kei Sato¹, OKUMURA, Motonori³, TOHNO, Susumu³

¹National Institute for Environmental Studies, ²Faculty of Environmental Earth Science, Hokkaido University, ³Graduate School of Energy Science, Kyoto University

Isoprene is the most abundant volatile organic compound (VOC) emitted from the earth and is producing a large amount of SOA by oxidation processes in the atmosphere. There are three oxidation processes for isoprene. The OH reaction is a major oxidation process in daytime. SOA yield and mechanism have been extensively investigated in many research groups so far. The NO₃ reaction occurs in night time. SOA yield of the O₃ reaction is known to be small compared with those of other reactions. The O₃ reaction occurs in both daytime and nighttime. Since the ozone reaction could couple with other oxidation processes, we think that it is important to understand the mechanism of SOA formation in the O₃ reaction. For the purpose, we detected semi-volatile organic compounds produced in the oxidation processes in both gaseous and aerosol phases by chemical ionization mass spectrometry that allows for sensitive measurement of VOC without any pretreatment.

The reaction was investigated using 6 m³ smog chamber. The initial concentrations of isoprene and ozone were fixed as 2 ppmv and 4 ppmv, respectively. In this reaction, OH radical is regenerated, so we did the experiments with OH radical scavenger. Cyclohexane and CO were used as an OH radical scavenger. The experiment was carried out under dry conditions and without sees particles. Gaseous reactants and products were monitored by FT-IR and proton transfer reaction-mass spectrometer (PTR-MS). SOA size distribution and concentration were monitored by Fast Mobility Particle Sizer (FMPS) within 10 minutes from the start of the reaction and Scanning Mobility Particle Sizer (SMPS) for the whole reaction time. After 2 hours, formed SOA was collected on three filters and was analyzed by PTR-MS, GC/MS and LC/MS. In addition to the smog chamber experiments, similar experiments were carried out using 1 m³ Teflon bag in order to compare PTR-MS data with negative ion-chemical ionization mass spectrometer (NI-CIMS) data.

Same ion signals were observed in both gaseous and aerosol phases by NI-CIMS and were assigned to oligomeric hydroperoxides involving Criegee intermediate (molecular weight 46) as a chain unit. PTR-MS detected the oligomeric hydroperoxides as [M-OH]⁺ ion. Since these compounds were observed in both gaseous and aerosol phases, it is concluded that they are key species for the SOA formation of isoprene ozonolysis. In SOA, hemiacetals involving formaldehyde (MW30) and/or MACR (MW70) were observed by PTR-MS. So, we found that the SOA formed in the isoprene ozonolysis consists of oligomeric hydroperoxides involving Criegee intermediate as a chain unit and hemiacetals involving formaldehyde and/or MACR.

Gas-aerosol partitioning of each VOC was estimated from ion signals in both gaseous and aerosol phases by PTR-MS. Gas-phase concentrations at each mass number were determined from mass spectrum observed after the reaction. Aerosol-phase concentrations were estimated from total ion signals summed during the heating of the filter. We assume that VOC is evaporated during the analysis time of 2 hours. From the ratio of aerosol-phase concentration to gas-phase concentration, we estimated saturation vapor pressures of compounds in the mass range between 100 and 200 to be approximately 10⁻⁴ Torr. On the other hand, from the fitting of SOA yield curve by four-product volatility basis model, model suggested that species 10⁻⁴ Torr of saturation vapor pressure are dominant in SOA. These are consistent with the compounds observed in the mass range between 100 and 200 and we assigned those as oligomeric hydroperoxides and hemiacetals.

Keywords: isoprene, ozonolysis, chemical ionization mass spectrometry, proton transfer reaction mass spectrometer, secondary organic aerosol, Criegee intermediate

Analysis of gas and particle phase products in the ethylene ozonolysis using negative ion chemical ionization mass spect

Yosuke Sakamoto^{1*}, HIROKAWA, Jun¹, Satoshi Inomata²

¹Faculty of Environmental Earth Science, Hokkaido University, ²Center for Global Environmental Research, National Institute for Environmental Scie

The reaction of ozone with alkenes is a significant loss process of both ozone and alkenes in the atmosphere and plays an important role in air pollution processes in urban areas. The alkene ozonolysis produces Criegee intermediates, which have relatively high reactivity and partly decompose to produce radicals such as OH, HO₂ and RO₂. Especially, the formation of OH in alkene ozonolysis can be important as a nighttime source of OH. Additionally, ozone-alkene reaction can contribute to the formation of secondary organic aerosols (SOAs). Despite of its importance, the reaction process of the ozone-alkene reaction is not fully understood. This is the case even in the ozonolysis of ethylene, which is the simplest alkene, widely used in industry, and one of the most significant volatile organic compounds (VOCs) released into the environment.

In this study, we investigated the ethylene ozonolysis in laboratory experiments with a Teflon bag by using negative ion chemical ionization mass spectrometry (NI-CIMS). NI-CIMS is a powerful tool with less fragment, high selectivity, and high sensitivity for analysis of compounds such as carboxylic acids and hydroperoxides, which are expected to be produced in the ethylene ozonolysis.

As gas-phase products, we detected oligomeric hydroperoxides composed of Criegee intermediates as a chain unit, as well as formic acid and hydroperoxides which are previously reported. Additionally, the formation of SOAs in the ethylene ozonolysis was observed and their components were analyzed using NI-CIMS. The oligomers composed of the Criegee intermediates were also found as particle components. The formation of gas-phase oligomers and SOAs was strongly suppressed by adding methanol as a Criegee scavenger, clearly indicating that the Criegee intermediate plays a main role in the formation of oligomers and SOAs in the ethylene ozonolysis. The sequential addition of Criegee intermediates to hydroperoxides was proposed as the oligomer formation mechanism.

Keywords: ozonolysis, ethylene, SOA, hydroperoxide, oligomerization

Mixing states of soot particles from transmission electron microscopy: their mixing state, size, shape, and composition

Kouji Adachi^{1*}, ZAIZEN, Yuji¹, Yasuhito Igarashi¹

¹Meteorological Research Institute

Mixing state, size, shape, and composition of atmospheric aerosol particles influence their climate and health effects. Transmission electron microscopy (TEM) can magnify the particles and reveal the internal structures at a single particle scale. We study aerosol particles collected from urban mountain sites in Japan. In this study, we focused on soot particles and their mixing states, shape, size, and compositions of the coating materials, if any, since they absorb light and have great influence on the climate.

Together with scanning transmission electron microscopy (STEM), which is one of the technique of TEM, and energy dispersive X-ray spectroscopy (EDS), which measures the composition of interest within TEM, we analyze the compositions and mixing states of soot particles as well as elemental distribution within individual particles. We use the STEM-EDS system that automatically measures sizes, shape factors, and compositions of all aerosol particles within a field of view (~300 particles). The results suggest that ~75% of soot particles were coated (internal mixture) at the mountain site (remote area) and the larger aerosol particles include the more soot particles. At the mountain site, soot particles were mostly coated by ammonium sulfate. On the other hand, soot particles from urban site were coated by both organic aerosol and sulfate, and the ratio varied depending on the time of the day. These data are useful to understand the optical properties, atmospheric lifetime, and climate effects of soot particles and to improve climate modeling.

Keywords: aerosol, electron microscope

Light absorption properties of carbonaceous particles in Nagoya

Tomoki Nakayama^{1*}, Yuka Ikeda¹, Yoshitaka Setoguchi², Yuki Sawada¹, Kaori Kawana², Michihiro Mochida², Yutaka Matsumi¹

¹Solar-Terrestrial Environment Laboratory and Graduate School of Science, Nagoya University, ²Graduate School of Environmental Studies, Nagoya University

Aerosol particles have an important role in radiation balance in the atmosphere by scattering and absorbing incident light. Black carbon (BC) particles are an important global warming agent with radiation forcing similar in magnitude to CO₂. The light absorption of BC is generally considered to be increased by internal mixing with other compounds but the amount of absorption enhancement depends on factors such as refractive index of BC and coating materials, size and location of the BC core (e.g. Bond et al. 2006). In addition, recently light-absorbing organic carbon "brown carbon", involving humic-like substance (HULIS) and nitro-aromatics etc., has been proposed as a source of significant absorption, particularly in the near-UV (e.g. Nakayama et al. 2012). However, observational studies of the enhancement of BC light absorption and brown carbon are still limited mainly because of the difficulty in the accurate measurement of light absorption of internally mixed BC particles without collecting on filter. In this work, by applying photoacoustic spectroscopy (PAS), light absorption enhancement of BC and contributions of light absorption by brown carbon is examined.

Observations were conducted during summer (August, 2011) and winter (January, 2012) at the Higashiyama-campus of Nagoya University. Absorption and scattering coefficients at 405, 532, and 781 nm of PM1 particles were measured using the photoacoustic soot photometer (DMT, PASS-3), after passing through diffusion dryers and one of the heaters controlled at 25, 100, and 300 degC (summer) or 25, 300, and 400 deg C (winter) every 30 (summer) or 10 (winter) min. Mass concentrations of elemental carbon (EC) and organic carbon (OC) were also measured by thermo-optical technique using a semi-continuous EC/OC analyzer (Sunset Lab., model 4) every 90 min.

By comparing absorption coefficients at 781 nm with and without heating (300 or 400 deg C), increase in BC light absorption due to coating was found to be small (<10 percent) both during winter and summer. The result is consistent with a recent observation by Cappa et al. (2012) conducted in California, USA. Contributions of light absorption by OC are estimated by assuming that the enhancement of BC light absorption due to coating does not depend on wavelength. As a results, contributions of 405 nm light absorption by OC, which is vaporized at 300 (or 400) deg C, are found to be small during summer in Nagoya (<5 percent) but significant (~20 percent) during winter. Larger absorption cross section of OC (MAC_{OC}) was observed especially when CO/ Δ -CO₂ ratio was higher. The result suggests that OC emitted from incomplete combustion processes such as biomass and coal burning for heating may contribute to the observed light absorption by OC during winter.

References

- Bond et al., J. Geophys. Res., 111, D202011 (2006).
- Cappa et al., Science, 337, 1078-1081 (2012).
- Nakayama et al., Earozoru Kenkyu, 27, 13-23 (2012).

Keywords: Aerosol optical properties, Ambient measurement, Black carbon, Lensing effect, Brown carbon, Climate change

Aging and long-range transport processes of black carbon: global simulation with a chemistry-aerosol climate model

Kengo Sudo^{1*}, Akihisa Wada¹, Toshihiko Takemura²

¹Graduate School of Environmental Studies, Nagoya University, ²Research Institute for Applied Mechanics, Kyushu University

Present global aerosol models generally have a severe tendency to underestimate atmospheric concentrations of black carbon (BC) especially in remote areas like the polar regions as shown by the recent model intercomparison project under the IPCC (ACCMIP/AeroCOM). Such underestimates of BC are basically coming from large uncertainties in aging process which makes hydrophobic BC to hydrophilic, and subsequent removal by precipitation. This problem in global BC modeling causes still a large uncertainty in the estimate of atmospheric heating and climate impacts of BC (Kerr, Science, 2013). This study attempted to improve global simulation of BC and re-evaluate radiative forcing of BC in the framework of a chemistry-aerosol coupled climate model MIROC-ESM-CHEM. Our previous study (Sudo and Endo, 2011) had successfully reproduced the concentration and seasonal cycle of BC observed at the Syowa station in the Antarctic, by applying a simplified aging scheme that considers coating of BC with SO_4^{2-} (Liu et al., 2011) to the MIROC-ESM-CHEM model. Our model, however, could not reproduce well the observed BC levels and seasonality in the northern high latitudes including in the Arctic. This study developed a new scheme to simulate more explicitly aging of BC associated with condensation of SO_4^{2-} and organic compounds from oxidation of VOCs. Additionally, several improvements were also added to the model for better simulating dry/wet deposition and emissions seasonality. Our improved model with the new aging scheme appears to relatively well reproduce the observed BC concentrations and seasonality in the Arctic region. Our simulation also showed that Arctic BC comes mainly from fossil fuel burning in winter to spring, but from the Siberian biomass burning in summer. The new model estimated radiative forcing of BC to be 0.83 W m^{-2} which is about two times larger than the estimate by our original model with no aging scheme (0.41 W m^{-2}), or the model ensemble mean in the IPCC report.

Keywords: black carbon, soot, aging, long-range transport, radiative forcing, global model

Seasonal variations of Asian black carbon outflow to the Pacific using a tagged three-dimensional model

Hitoshi MATSUI^{1*}, Makoto Koike¹, Yutaka Kondo¹, Naga Oshima², Nobuhiro Moteki¹, Yugo Kanaya³, Akinori Takami⁴, Martin Irwin¹

¹University of Tokyo, ²Meteorological Research Institute, ³Japan Agency for Marine-Earth Science and Technology, ⁴National Institute for Environmental Studies

The Community Multiscale Air Quality model with a source and process tagged method (CMAQ/PASCAL) was used to understand source regions and types (anthropogenic (AN) and biomass burning (BB)) of Asian black carbon (BC) outflow to the Pacific during 2008 - 2010. The model calculations generally reproduced absolute concentrations and temporal (seasonal, monthly, and day-to-day) variations of BC mass concentrations observed by both surface and aircraft measurements in outflow regions in East Asia. These model calculations show that both the total eastward flux and transport efficiency (fractions transported from sources) of BC are the highest during spring (26 kg s⁻¹ and 33% at 150E) and the lowest during summer (8 kg s⁻¹ and 20% at 150E). These seasonal variations of Asian BC outflow are generally controlled by transport patterns (monsoons, frontal passages, and convection) and emissions from the following three sources: (1) AN emissions from China (China AN), (2) BB emissions from Southeast Asia and South China (SEA BB) during February - April, and (3) BB emissions from Siberia and Kazakhstan (Siberia BB) during April - July. In our calculations, China AN dominates the total eastward BC flux on period average (61%, 17%, and 6% from China AN, Siberia BB, and SEA BB, respectively, at 150E). On the other hand, SEA and Siberia BB account for 30 - 50% of the total eastward BC flux (150E and 175E) during spring and summer, and they intensify seasonal contrast of Asian BC outflow flux. BC from Siberia BB is also found to be transported to the Pacific more efficiently than that from other sources. Although the amounts of BB emissions are currently highly uncertain, our results suggest that the control of Siberia BB will be important in terms of the trans-boundary transport of BC to the Pacific, North America, and the Arctic.

Keywords: black carbon, regional three-dimensional model, tag model, East Asia, source contribution, biomass burning

Vertical transport mechanisms of black carbon over East Asia in spring during the A-FORCE aircraft campaign

Naga Oshima^{1*}, Makoto Koike², Yutaka Kondo², Hitoshi MATSUI², Nobuhiro Moteki², Hisashi Nakamura³, Nobuyuki Takegawa³, Kazuyuki Kita⁴

¹Meteorological Research Institute, ²Department of Earth and Planetary Science, Graduate School of Science, The University of Tokyo, ³Research Center for Advanced Science and Technology, The University of Tokyo, ⁴Faculty of Science, Ibaraki University

Black carbon (BC) aerosols efficiently absorb solar radiation in the atmosphere. The absorption leads to heating of the atmosphere and melting of some additional snow or sea ice, therefore exerting a substantial impact on radiation budget in the climate system. The vertical transport processes of BC from the planetary boundary layer (PBL) to the free troposphere (FT) are critically important, because they directly control the global- and regional-scale spatial distributions of BC; however an understanding of this process is still limited. In order to understand these points, the Aerosol Radiative Forcing in East Asia (A-FORCE) aircraft campaign was conducted over East China Sea and Yellow Sea in March-April 2009 and 120 vertical profiles of BC were obtained at 0-9 km in altitude. The major objective of this study is to understand the vertical transport mechanisms of BC particles and their transport pathways over East Asia in spring using results from the 3-D chemical transport model (WRF-CMAQ) calculations and the A-FORCE observation data.

The original CMAQ model does not take into account differences in rainout and washout processes. In this study, we modified the CMAQ model to treat rainout and washout processes separately. We conducted the WRF-CMAQ model calculations with horizontal resolution of 81 km * 81 km and with 21 layers in vertical, and used the model results in March-April 2009. We also estimate transport efficiency of BC on the basis of the calculation with wet deposition and that without wet deposition using the modified CMAQ model.

Comparisons of the model results with the A-FORCE observations show that the model reproduces relatively well the vertical distributions of mass concentration and transport efficiency of BC, including dependences on precipitation that air parcels had been experienced during transport, although the model overestimated the mass concentrations of BC in the FT.

Using the validated model results during the A-FORCE period (20 March to 30 April 2009), we find that the pronounced convergences of mean horizontal mass fluxes of BC integrated within the PBL (700-1000-hPa column) over northern-eastern and inland-southern (around the high-altitude mountains) China. Corresponding to the convergence areas, we find two types of the pronounced upward mass fluxes of BC from the PBL to the FT (at the 700-hPa level) over northern-eastern and inland-southern China. The major uplifting mechanism of BC over northern-eastern China is cyclones with modest amounts of precipitation. In addition to cumulus convections, orographic lifting along the high-altitude mountains plays important role for the upward transport of BC to the FT over inland-southern China, in spite of the largest wet deposition amounts of BC in East Asia due to large amounts of precipitation. The latitudinal difference of precipitation induced by the moisture supply by the low-level southerlies is responsible for the spatial distributions of BC and its transport efficiency in the atmosphere.

The mean eastward mass fluxes of BC were pronounced in the lower troposphere over the midlatitude region (35°-50N) and in the middle troposphere over the subtropical region (20°-35N) at the 140E vertical cross section during the A-FORCE period. We find that the upward transports over northern-eastern and inland-southern China, followed by the westerly transports in the lower and the middle FT, respectively, make major contributions to the exports of BC from East Asia to the Pacific in spring.

Keywords: Aerosol, Black carbon, Transport, Wet deposition, East Asia, Regional-scale aerosol model

Corona-imaging colorimetric method for accurate measurement of the size of water droplets in an expansion chamber

Hiroka Aoki^{1*}, Nobuhiro Moteki¹, Yutaka Kondo¹

¹Graduate School of Science, The University of Tokyo

Accurate and time-resolved measurement of the size of water droplets is a pre-requisite for the study of microphysical processes of cloud formation using an expansion chamber. We developed a new method using color images of corona observed under illumination of a white-light beam, also known as the corona-imaging colorimetry (CIC) method. In the CIC method, RGB data from images obtained by a commercial digital camera are converted into standard colorimetric parameters. The droplet size is estimated by optimizing the agreement of the measured colorimetric parameters with those estimated using Mie theory. For polystyrene latex spheres suspended in water, the particles size estimated by the CIC method agrees to within 2% of the pre-determined value. We apply this method to the time-resolved measurement of the size of water droplets formed in an expansion chamber. The CIC method is technically simple and enables accurate and instantaneous measurements of the size of droplets with diameters larger than about 10 μm . In addition, the CIC method is advantageous over the Constant Angle Mie Scattering (CAMS) method, which requires a specially designed optical system with a laser light source and complete information of the growth history of the droplets.

In our presentation, the details of the theoretical aspects and colorimetric treatments of the CIC method will be discussed.

Keywords: Corona, Cloud Droplets, Sizing, Chamber, Condensation

Influences of near-surface stratification for aerosol impact on clouds over the East China sea

Makoto Koike¹, Nobuyuki Takegawa^{2*}, Nobuhiro Moteki¹, Yutaka Kondo¹, Hisashi Nakamura²

¹Graduate School of Science, The University of Tokyo, ²Research Center for Advanced Science and Technology, The University of Tokyo

Cloud microphysical properties and aerosol concentrations were measured aboard an aircraft over the East China Sea and Yellow Sea in April 2009 during the Aerosol Radiative Forcing in East Asia (A-FORCE) experiment. We sampled stratocumulus and shallow cumulus clouds over the ocean in 9 cases during 7 flights 500-900 km off the east coast of Mainland China. Cloud droplet number concentration (highest 5%, N_{c_max}) correlates well with the accumulation-mode aerosol number concentration (N_a) below the clouds. N_{c_max} correlates partly with near-surface stratification evaluated as the difference between the sea surface temperature (SST) and 950-hPa temperature ($SST - T_{950}$). Cold air advection from China to the East China Sea was found to bring not only a large number of aerosols but also a dry and cold air mass that destabilized the atmospheric boundary layer, especially over the warm Kuroshio ocean current. Over this high-SST region, greater updraft velocities and hence greater N_{c_max} likely resulted. We hypothesize that the low-level static stability determined by SST and regional-scale airflow modulates both the cloud microphysics (aerosol impact on clouds) and macro-structure of clouds (cloud base and top altitudes, hence cloud liquid water path).

Keywords: aerosol, cloud, SST, Kuroshio Ocean current, East Asia

Characteristics of cloud condensation nuclei observed at Noto peninsula, Japan, in autumn 2012

Yoko Iwamoto^{1*}, Kento Kinouchi², Atsushi Matsuki¹

¹Institute of Nature and Environmental Technology, Kanazawa University, ²College of Science and Engineering, Kanazawa University

Atmospheric aerosols can act as cloud condensation nuclei (CCN) and therefore play an important role in regulating radiative properties and lifetime of clouds. Along with the development of the industrial activities, the loading of atmospheric aerosols tends to increase, especially in East Asia. To access the radiative balance and/or hydrological cycle of the Earth in the future, quantitative evaluations of CCN characteristics are needed based on in-situ atmospheric observations.

In this study, CCN activity of submicrometer-sized aerosols were measured at Noto Ground-based Research Observatory (NOTOGRO), located at the tip of Noto peninsula, facing the Sea of Japan, in autumn 2012. Ambient aerosols were sampled through the PM10 inlet (14.7 m A.G.L.). The dried aerosols were introduced into a differential mobility analyzer (DMA) for size selection, and the resulting monodisperse aerosol was then transferred to a water-based condensation nuclei (CN) counter and a continuous flow thermal gradient CCN counter to measure the number concentrations of CN and CCN, respectively. The CCN efficiency spectra, where CCN number fraction is plotted against the diameter of aerosols, were obtained at four different supersaturations (0.1%, 0.2%, 0.5% and 0.8%). The bulk chemical composition of non-refractory submicrometer-sized aerosols was also measured by an aerosol chemical speciation monitor (ACSM).

Parameters related to the mixing state and hygroscopicity of the aerosols were obtained at high time resolution based on the analysis of the CCN efficiency spectra. The slope of the CCN efficiency spectra (diameter at which 50% of CN act as CCN) for ambient aerosols was not as steep as that for pure ammonium sulfate particles, indicating heterogeneity in the mixing states of the ambient aerosol. The hygroscopicity parameter κ (Peters and Kreidenweis, 2007), estimated from the CCN activation diameter, suggested that organics contributed on the aerosol mass especially in the size range of less than 100 nm. The bulk chemical composition obtained by ACSM also indicated the large contribution of organics on the total aerosol mass, however, the size resolved CCN measurements provided a clue to the elucidation of the size-dependant chemical composition of submicrometer-sized aerosols.

References:

Peters and Kreidenweis (2007), *Atmos. Chem. Phys.*, 7, 1961-1971.

Keywords: atmospheric aerosols, cloud condensation nuclei, organic aerosols, hygroscopicity parameter, East Asia

Cloud droplet size measured for different supersaturations at Noto Peninsula, Japan, in autumn 2012.

Kento Kinouchi^{1*}, Yoko Iwamoto², Atsushi Matsuki²

¹School of Graduate School of Natural Science & Technology, Kanazawa University, ²Institute of Nature and Environmental Technology

The size of cloud droplets is one of the important factors that control the radiative properties and lifetimes of clouds. In general, it has long been accepted that growth rates of cloud droplets depend solely on water vapor supersaturation (SS). To challenge this established theory, we conducted in-situ measurement of atmospheric aerosols and related cloud growth kinetics in East Asia, in order to investigate the relative importance of other factors that can potentially influence the initial cloud droplet growth. In this study, diameters of cloud droplets were measured by using cloud condensation nuclei counter (CCNC) at Suzu, Noto Peninsula (NOTOGRO) in October, 2012. CCNC was operated at four different SS conditions (SS=0.1%, 0.2%, 0.5%, 0.8%). The diameters of cloud droplets activated from ambient aerosols were compared to those activated from ammonium sulfate (regarded here as representative inorganic CCN). The negative correlations between the cloud droplets' diameters and organic aerosol mass fractions were observed. The initial growth rate of cloud droplets activated from ambient aerosol were considered to be inhibited by the existence of organics especially under the lower SS conditions (SS=0.1% and 0.2%).

Keywords: cloud condensation nuclei, cloud droplet size, atmospheric aerosol, chemical composition

SMILES measurements of diurnal variations of hydroperoxyl radical (HO_2) in the stratosphere and mesosphere

Nao Suzuki^{1*}, Hideo Sagawa², Yukio Nakano¹, Nori Mizuno², Yasuko Kasai²

¹Tokyo Gakugei University, ²NICT

1 Introduction

HO_2 radical is among the most important oxidants for atmospheric chemical compositions in the upper atmosphere. The accurate measurement of HO_2 turned out to be an extremely difficult problem because HO_2 volume mixing ratios are about a few parts per billion by volume. No significant measurement was reported so far to evaluate the atmospheric chemistry of HO_2 such as its diurnal variations and behaviors in stratosphere and mesosphere.

In this study, we report the first wide altitude range observations from stratospheric to mesospheric HO_2 diurnal variations, the measurements of which were previously considered to be difficult, by Superconducting Submillimeter-Wave Limb-Emission Sounder (SMILES). We discuss hydrogen chemistry in the stratosphere and mesosphere.

SMILES is a part of Japanese Experiment Module (JEM) onboard International Space Station (ISS).

2 Dataset and Analysis of SMILES HO_2 measurements

ISS which has SMILES platform orbits at an altitude of 320-340 km above the surface and completes a single earth orbit in about 90 minutes. SMILES observed about 1630 points per day over the Earth during September 2009-April 2010, and produce a global map everyday for each composition. The latitudinal range of the observation covers from 65° N to 38° S.

SMILES detects thermal emission from chemical substances contained in the atmosphere and obtains the emission signal from atmospheric compositions at the several height in the atmosphere. HO_2 transition frequency is 649.70 GHz.

We have used HO_2 data from SMILES NICT products. We selected the data into three parts of latitude. These parts are equator (20° N-20° S), mid-latitude (20° N-50° N) and north polar (50° N-65° N), respectively. And we selected HO_2 vertical profiles at 20-95 km at night and in the daytime and HO_2 diurnal variations as a function of solar zenith angle (SZA) at 10° intervals in the stratosphere (29.0-49.0 km) and mesosphere (53.0-74.5 km), in each region of latitude.

3 Results and Discussions

HO_2 vertical profiles at 20-95 km are obtained. HO_2 volume mixing ratios generally increase with the altitude above 20 km and the appearance of the maximum (peak) volume mixing ratio in the profile is evident in the mesosphere, near 79.5 km at about 3ppbv at night and near 74.5 km at about 5.5ppbv in the daytime. We confirmed that the altitude of daytime peak in the shape of HO_2 profiles is lower than that of nighttime peak in all parts of latitude.

The diurnal variation of HO_2 through in the stratosphere and mesosphere was obtained for the first time (Figure 1). HO_2 volume mixing ratios at the all altitude are enhanced during the daytime due to photochemical reaction. The largest source of HOx (= H + OH + HO_2) radicals in the stratosphere are provided from reaction $\text{O}(^1\text{D})$ atoms, which are generated predominantly from O_3 photolysis, with H_2O .

The increase of HO_2 mixing ratios in the stratosphere with altitude can largely be attributed to an increased formation rate due to the large increase in the abundance of $\text{O}(^1\text{D})$ at high altitude in the stratosphere. On the other hand, the production processes for mesospheric HOx during the daytime involve the photodissociation reaction of water vapor, which plays an important role in HO_2 production additionally in the mesosphere.

Acknowledgements: Data processing and other research works in the present study was performed with the NICT Science Cloud at National Institute of Information and Communications Technology (NICT) as a collaborative research project.

Keywords: oxidant, HO_2 , hydroperoxyl radical, diurnal variation, stratosphere, mesosphere

AAS21-P01

Room:Convention Hall

Time:May 19 18:15-19:30

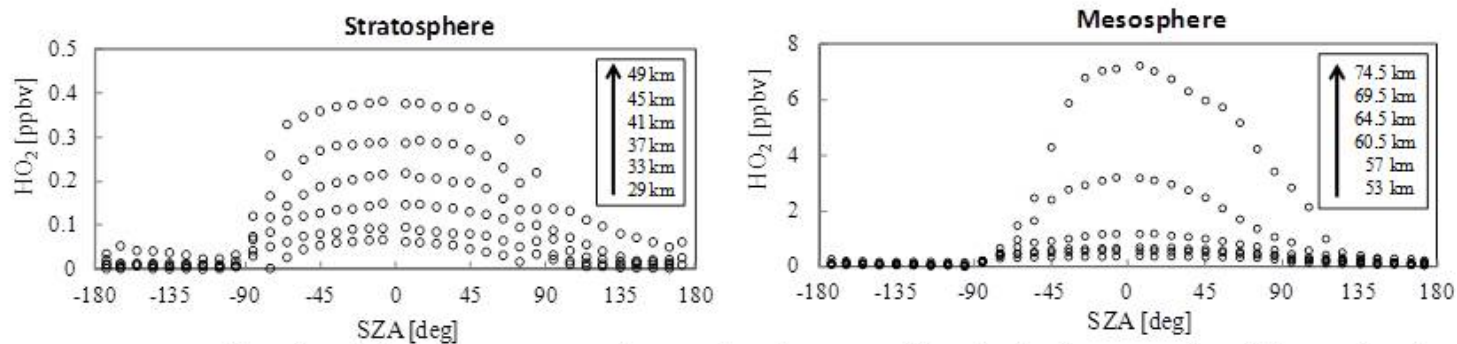


Figure 1. HO₂ diurnal variations from SMILES observations for equatorial region in the stratosphere (left panel) and mesosphere (right panel) at the altitude from 29.0 km up to 74.5 km.

Impacts of the Arctic ozone depletion on Japan observed with FTIR between 2009 and 2011

yuki hashimoto^{1*}, Isao Murata¹, Hideaki Nakajima², Isamu Morino²

¹Tohoku University, ²National Institute for Environmental Studies

The ozone depletion is one of the environmental problems. In 2011, ozone depletion which was comparable to the Antarctic ozone hole occurred in the Arctic.

The ozone depletion has occurred inside the polar vortex. The air mass from inside the polar vortex is spread to mid-latitude in spring after its breakup. The purpose of this study is to quantify the impact of polar ozone depletion on mid-latitude by comparing the amounts of ozone in mid-latitude air masses before and after the breakup of the polar vortex.

Vertical profiles of ozone and hydrogen fluoride (HF) have been retrieved from infrared spectra observed with a Fourier transform infrared spectrometer (FTIR) at Tsukuba using the SFIT2 spectral fitting program developed by Rinsland et al. [1998].

HF can be used as a tracer of the transport, because HF is a remarkably stable species in the stratosphere. Ozone and HF usually show a very high correlation in the lower stratosphere because both species are stable. But the correlation will be changed when ozone is chemically perturbed. Therefore, we examined the correlations of mixing ratios between ozone and HF in the mid-latitude air masses before and after the breakup.

Goto et al. [2010] compared the ozone-HF mixing ratio correlations in the mid-latitude air masses before and after the breakups of the polar vortex between 2005 and 2008 and indicated that ozone was decreased by 0.2 to 0.4 ppmv at around 19km altitude in 2007 and 2008. Preliminary analysis in 2009 shows no impact of the ozone depletion at Tsukuba. We report the impacts of the Arctic ozone depletion on Japan between 2009 and 2011.

Simulation study of synergetic retrieval for tropospheric ozone with UV, TIR, and MW measurements

Takao M. Sato^{1*}, Hideo Sagawa², Hitoshi Irie³, Katsuyuki Noguchi⁴, Naoko Saitoh³, Ryoichi Imasu⁵, Yoji Hayashi⁵, YASUKO KASAI²

¹Institute of Space and Astronautical Science, Japan Aerospace Exploration Agency, ²National Institute of Information and Communications Technology, ³Center for Environmental Remote Sensing, Chiba University, ⁴Nara Women's University, ⁵CCSR, The University of Tokyo

Tropospheric ozone, one of short-lived climate pollutants (SLCPs), plays an important role on climate change, atmospheric chemistry, and air quality. First, ozone acts a greenhouse gas, especially in the upper troposphere (UT) and its effect is the strongest near the tropopause where the climate system is more sensitive. Second, ozone in the planetary boundary layer (PBL) is known to be a major component of photochemical smog and causes severe damages the health of both plants and animals. Finally, ozone has an oxidizing capability to remove many pollutants (e.g., methane and carbon monoxide) from the atmosphere. In order to understand these processes of tropospheric ozone with the aid of numerical model calculations, it is essential to monitor the global distribution of tropospheric ozone with a fine vertical resolution. However, current available remote sensing instruments, which measure backscattered solar UV radiance (e.g., Aura/OMI) and thermal infrared emission (e.g., Aura/TES), cannot resolve tropospheric ozone alone.

For the purpose of improving the current capability of tropospheric ozone retrieval, we have proposed a new atmospheric remote sensing equipment named Air Pollution Observation (APOLLO) to be carried aboard the Japanese Experiment Module (JEM) on the International Space Station (ISS). APOLLO is planned to carry two nadir-viewing passive instruments (UV+VIS and TIR) and one limb-viewing microwave passive instrument (MW), which are dedicated to measure tropospheric ozone and its precursors relating to air quality with high spatial resolution (~2 km) and high vertical resolution (the requirement is to divide troposphere into three layers: UT, LT (lower troposphere), and PBL).

In this study, we investigate synergetic effect of combination of UV, TIR, and MW measurements on retrieval sensitivity of tropospheric ozone. We evaluate the retrieval sensitivity to tropospheric ozone profile with Optimal Estimation Method (OEM) [Rodgers, 2000]. Twenty atmospheric scenarios generated from a global-regional chemical transport model system are used as true profiles for this aim. The combination of UV and TIR measurements improves values of the degree of freedom for signal (DOFS) in PBL. MW limb measurements provide significant information on UT and the stratosphere. We find that adding MW limb measurements to UV+TIR measurements significantly improve values of DOFS in PBL, although MW limb measurements alone are not sensitive to PBL. We conclude that this is because UV+TIR measurements become more sensitive to PBL by adding MW limb measurements which can reduce the uncertainty of ozone concentration in UT compared with that from UV+TIR measurements.

Keywords: International Space Station, Tropospheric ozone, Multispectral observations

Improvement of retrieval algorithm of CO₂ and CH₄ profiles from GOSAT/TANSO-FTS TIR band

Naoko Saitoh^{1*}, IMASU, Ryoichi²

¹Center for Environmental Remote Sensing, Chiba University, ²Atmosphere and Ocean Research Institute, The University of Tokyo

The Greenhouse Gases Observing Satellite (GOSAT), which was developed by the National Institute for Environmental Studies (NIES), the Ministry of the Environment (MOE), and the Japan Aerospace Exploration Agency (JAXA), has been observing greenhouse gases continuously for about four years since its launch on January 23th, 2009. GOSAT consists of four spectral bands: three of the four bands in shortwave infrared (SWIR) region and one in thermal infrared (TIR) region. GOSAT can simultaneously observe CO₂ and CH₄ column-averaged dry-air mole fractions and their profiles in the same field of view from the SWIR and TIR bands. TIR Version 00.01 Level 2 (L2) data have been released to the public. The V00.01 L2 data were processed with a previous version (V100.100) of Level 1B (L1B) data. Although a single TIR V00.01 L2 CH₄ profile does not have enough quality for scientific use, the TIR column-averaged CH₄ value agrees to aircraft CH₄ data within 0.5% [Saitoh et al., 2012]. On the other hand, TIR V00.01 L2 CO₂ data do not have enough quality; they show a relatively large variability and have a clear bias in mid-troposphere in low latitudes. This study improves an algorithm for retrieving CO₂ and CH₄ profiles from TIR band. The new algorithm simultaneously retrieves several parameters other than target gases such as CO₂ and CH₄. The TIR retrieval processing in this study uses the latest version of L1B data; therefore, L2 data bias attributed to L1B spectral bias would be expected to decrease.

Keywords: greenhouse gas, satellite remote sensing, retrieval algorithm

The temporal variation of vertical profile of methane at Poker Flat observed by Fourier transform spectrometer

Koichi Maruno¹, Isao Murata^{2*}, YASUKO KASAI³, Kagwa Akiko⁴, Yasumasa Kasaba¹

¹Graduate school of science, Tohoku University, ²Graduate school of environmental studies Tohoku University, ³National Institute of Information and Communications Technology, ⁴FUJITSU FIP CORPORATION

Methane is the second important greenhouse gas. In the arctic region, there are many sources of the atmospheric methane, i.e., wetlands, permafrosts and natural gas fields. It is important to investigate the trend of the methane in the arctic region.

In this study, we analyzed the trend of the vertical profile of methane at Poker Flat (Latitude: 65.11 N, Longitude: 147.42 W) observed with FTIR (Fourier Transform Infrared Spectrometer) by NICT from 2000 to 2010 (except for 2006). The vertical profiles of methane were derived with the SFIT2 spectrum fitting program using Rodgers' Optimal Estimation Method (OEM).

We investigated temporal variation of the columns in the lower stratosphere (10-21 km), troposphere (0-10 km), and total (0-100 km) which calculated from the vertical profiles with digital fitting method [Nakazawa *et al.*, 1997]. Lower stratospheric column shows no significant trend. Tropospheric and total columns show increase in 2008 then decrease in 2009. This trend in the troposphere is different from those observed in Germany, East Asia and Global average which don't show decrease after 2008. The difference of the trend indicates that observations at various regions are important in order to understand the spacial and temporal variations of sources and sinks of methane.

Keywords: methane, FTIR(Fourier transform Infra-Red spectrometer)

Optimization of wavenumber regions for the retrieval of the vertical profiles of CH₄ from infrared spectra

Isao Murata^{1*}, Hideaki Nakajima², Isamu Morino²

¹Graduate School of Environmental Studies, Tohoku University, ²National Institute for Environmental Studies

CH₄ is the second important greenhouse gas but there is large variability of its increasing rate that may be due to variabilities of sources. Therefore, it is important to investigate the vertical profile of CH₄.

Solar infrared spectra have been observed with a Fourier transform spectrometer (FTS) at Tsukuba, Japan. FTS has advantages in its high-resolution and the wide wavenumber range. Vertical profiles of some species can be derived from the high-resolution spectra with the SFIT2 spectral fitting program developed by Rinsland et al. (1998). It needs to select appropriate wavenumber regions and the optimization of fitting parameters is also needed. Now we are investigating these wavenumber regions and parameters in the NDACC/IRWG group for the retrieval of the vertical profiles and column densities of CH₄. Sussmann et al. [2011] analyzed with some combinations of the following wavenumber regions: 1) 2613.7 - 2615.4 cm⁻¹, 2) 2650.6 - 2651.3 cm⁻¹, 3) 2835.5 - 2835.8 cm⁻¹, 4) 2903.6 - 2904.03 cm⁻¹, 5) 2921.0 - 2921.6 cm⁻¹, and reported the combination of 1), 3), and 5) is best. We also compared the results from some combinations of these wavenumber regions and found that the discrepancy become large in summertime. It may be due to HDO absorption lines existing in these wavenumber regions as an interfering species.

Keywords: FTIR, Trace Species, Methane

Temperature from GPS RO meas. correlative to satellite and airborne obs. for comparing those CH₄ profiles

Takafumi Sugita^{1*}, Naoko Saitoh², Sachiko Hayashida³

¹NIES, ²Chiba Univ., ³Nara Women's Univ.

Evaluations of data quality of CH₄ retrieved from satellite-borne nadir sensors, from which are ADEOS/IMG in 1996-97, MetOp-A/IASI from 2007, and so on, in the troposphere and stratosphere have been performed in recent years (e.g., Clerbaux et al., ACP, 2003; Xiong et al., Remote Sens., 2010; Wecht et al., ACP, 2012; Razavi et al., ACP, 2009). GOSAT/TANSO-FTS started its operation from 2009, expected contributions in this area. For retrieving CH₄ profiles, it is necessary to input several external parameters such as temperature profiles, surface temperature, emissivity, and so on. A purpose of this paper is to understand the effect of temperature profiles on the CH₄ retrieval in the thermal infrared band of TANSO-FTS. So that, we will prepare temperature profiles from GPS radio occultations (RO). We will focus on GOSAT observations in the northern high-latitudes, where aircraft observations have been done by National Institute for Environmental Studies with the aid of Russian Academy of Science. We extracted data from coincidences between two Russian aircraft sites and GOSAT since 2009. Then, the RO temperatures for those pairs are prepared and compared with some meteorological datasets.

Keywords: temperature, methane, GPS, GOSAT, aircraft

Shipboard measurements of atmospheric CH₄, CO₂ and CO mixing ratios during the MR12-E03 cruise of the R/V Mirai

Yasunori Tohjima^{1*}, SASANO, Daisuke², ISHIDOYA, Shigeyuki³, KATSUMATA, Keiichi¹, MATSUSHITA, Junji¹, Kentaro Ishijima⁴, Prabir Patra⁴

¹National Institute for Environmental Studies, ²Meteorological Research Institute, ³National Institute of Advanced Industrial Science and Technology, ⁴Japan Agency for Marine-Earth Science and Technology

In order to investigate the potential sources of methane (CH₄) in the Arctic region, continuous measurements of the atmospheric CH₄ were carried out during a R/V Mirai Arctic Ocean cruise from September 3 to October 17, 2012. A cavity ring-down spectroscopy (CRDS) analyzer was used for the shipboard measurements of the atmospheric CH₄, carbon dioxide (CO₂) and carbon monoxide (CO). The analytical precisions evaluated from the measurements of the standard gases at a 24-hour interval during the cruise were 0.02 ppm, 0.3 ppb, and 0.9 ppb for the 5-min averages of CO₂, CH₄, and CO mixing ratios, respectively. When the wind blew from the relative direction of 200 +/- 20 degrees (rear left of the vessel), the contamination caused by its own exhaust fumes affected the CO₂ and CO mixing ratios with a tight correlation ($\Delta_{CO}/\Delta_{CO_2}=3.8$ ppb/ppm), while there was no significant influence from the exhaust fumes on the CH₄ mixing ratio. Such pollution events are easily distinguishable by the characteristics of the relative wind direction, the tight correlation of CO vs. CO₂, and large short-term (~a few second) variability. The observed CH₄ mixing ratios showed larger variations with elevated peaks of several tens ppb in the Bering Strait, Chukchi Sea, and Arctic Ocean (65-75°N, 155-175°W) in comparison with in the western North Pacific. The largest CH₄ peaks of about 50 ppb were observed off the northern Alaskan coast. Since these CH₄ peaks were associated with similar CO₂ peaks but not with CO peaks, it is unlikely that the combustion processes or ocean were the sources of the elevated CH₄. The backward trajectory analysis suggests that the North Slope of Alaska is the most probable CH₄ source region. The simulated CH₄ variations based on an atmospheric transport model and given flux maps well capture the observed CH₄ variations, also suggesting that the most of elevated CH₄ were derived from the land sources.

Keywords: atmospheric CH₄, the Arctic Ocean, cavity ring down spectroscopy analyzer (CRDS), shipboard measurements

Carbon monoxide and ozone measurements during summertime at the summit of Mt. Fuji

Shungo Kato^{1*}

¹Tokyo Metropolitan University

The top of Mt. Fuji is 3776 m and it located in free troposphere. Mt. Fuji weather station is a unique observatory for atmospheric measurements of free troposphere. But now the weather station is only open during summer. At the summit of Mt. Fuji, O₃ has been observed from 2007, and CO has been observed from 2008 during summer season.

CO and O₃ are monitored by Thermo Environmental Instrument Model 48C and 49i, respectively. Before and after the summertime intensive measurements, these instruments were calibrated by standard gas. Since CO analyzer is influenced by temperature and water vapor concentration, zero air produced by heated Pt catalyst was measured periodically.

Observed CO and O₃ concentrations showed large variation compared to other remote sites. Basically, CO and O₃ showed similar concentration change because clean air with low concentration and polluted air with high concentration are arrived to Mt. Fuji time to time. When only CO was high, polluted air experienced less photo chemical activity was arrived. When only O₃ was high, air from upper troposphere with high O₃ was arrived. Scatter plot of CO and O₃ was categorized by water vapor. Clear trend of low water, high O₃ and low CO was observed.

Low water vapor but high CO was observed in some case. It is expected that polluted air was lifter up and transported to the observatory.

Diurnal variation of CO and O₃ were not observed clearly. The influence of mountain wind is not important at least for CO and O₃.

The average concentrations of CO and O₃ for each year have large difference year to year. Influence of clean ocean air mass and polluted continental air mass will be different for each year and it affected the average concentration of pollutants during summer.

Keywords: free troposphere, longrange transport, mountain site, high altitude

A decadal inversion of carbon dioxide using the Global Eulerian-Lagrangian Coupled Atmospheric model (GELCA)

Tomoko Shirai^{1*}, Misa Ishizawa¹, Ruslan Zhuravlev², Alexander Ganshin², Tazu Saeki¹, Dmitry Belikov¹, Tomohiro Oda³, Makoto Saito⁴, Vinu Valsala⁵, Shamil Maksyutov¹

¹National Institute for Environmental Studies, ²Central Aerological Observatory, ³NIES, now at CSU/NOAA ESRL, ⁴NIES, now at LSCU, ⁵NIES, now at ITTM

A decadal estimate of global CO₂ flux distribution for the period of 2001-2010 was conducted using an atmospheric inversion modeling system called GELCA (Global Eulerian-Lagrangian Coupled Atmospheric model) with Kalman smoother inversion technique. The use of Lagrangian particle dispersion model (LPDM) to simulate the transport in the vicinity of the observation points enables us to avoid numerical diffusion from which Eulerian models suffer, and is suitable to represent observations at high spatial and temporal resolutions. An Eulerian model is run to generate the global background concentrations to be used as the boundary conditions for an LPDM that performs backward simulations from each receptor point (observation location). In GELCA, National Institute for Environmental Studies-Transport Model (NIES-TM) version 8.1i was used as an Eulerian global transport model coupled with FLEXPART version 8.0 as a LPDM. Two-day backward transport by FLEXPART was combined with the background CO₂ levels 2 days prior to the observations simulated by NIES-TM. The meteorological data for driving both models was taken from JMA Climate Data Assimilation System (JCDAS) with a spatial resolution of 1.25° x 1.25° and a temporal resolution of 6 hours. Our prior CO₂ fluxes consist of the following four types: daily terrestrial biospheric fluxes generated by the VISIT model (Vegetation Integrative Simulator for Trace gases); monthly oceanic fluxes generated by an ocean pCO₂ data assimilation system; monthly biomass burning emissions taken from the Global Fire Emissions Database (GFED), version 3.1; and monthly fossil fuel emissions combining the high-resolution Open source Data Inventory of Anthropogenic CO₂ emission (ODIAC) version 3.0 dataset. We employed a Kalman Smoother inversion technique with fixed lag of 3 months, solving for 42 land and 22 ocean regions.

The purpose of the present study is to evaluate the performance of the GELCA inversion system with rather long period (10 years) CO₂ flux estimation and to examine the impact of observation network. We tested several different sets of observation datasets starting by using the NOAA flask network ground based observations as a control case. The sensitivity of the inversion to the choice of CO₂ observation dataset was discussed using the footprint of each observation dataset. The CO₂ flux estimate was examined in terms of observation network/coverage and also compared with previous studies.

Keywords: CO₂, sources/sinks, inverse modeling, coupled model

Trends and seasonal cycle of atmospheric radiocarbon in carbon dioxide observed at Hateruma Island

Yukio Terao^{1*}, Hitoshi Mukai¹

¹Center for Global Environmental Research, National Institute for Environmental Studies

We have been conducted monthly air samplings for measurements of atmospheric radiocarbon in carbon dioxide ($^{14}\text{CO}_2$) at Hateruma Island (HAT, 24.05N, 123.80E, 47 m a.s.l.), Japan since 2004. We collected whole air samples using 2.0L glass flasks pressurized to 3 atm, and 5L air was used for radiocarbon analysis. The values of Delta14C were measured using compact Carbon Accelerator Mass Spectrometry (CAMS, NEC 1.5SDH). Uncertainty in Delta14C measured by CAMS is less than 2 per mil, which is based on the number of ^{14}C counts and the scatter of $^{14}\text{C}/^{12}\text{C}$ ratios during measurements. The reproducibility of CAMS measurements is ± 1.4 per mil (standard deviation of Delta14C values in a reference air cylinder).

Here we show the Delta14C values of background maritime air observed at HAT from 2004 to 2012. The seasonal cycle of Delta14C was observed: minimum in winter-spring and maximum in summer, with amplitude of 10 per mil. Decreasing trends in Delta14C were from -5 to -6 per mil/year, however, higher growth rates (less decreasing trends) of -2 per mil/year were observed in 2008-2009. The reason for the IAV in Delta14C will be discussed.

Keywords: carbon cycle, carbon isotope measurements, accelerator mass spectrometry

Long-term measurements of black carbon concentrations in rainwater at a remote site in East Asia

Tatsuhiko Mori^{1*}, Sho Ohata¹, Yutaka Kondo¹, Nobuhiro Moteki¹, Hitoshi Matsui¹, Aya Iwasaki², Nobutaka Tomoyose², Hisashi Kadena²

¹Graduate School of Science, University of Tokyo, ²Okinawa Prefectural Institute of Health and Environment

Black carbon (BC) particles are mainly emitted into atmosphere by incomplete combustion of fossil fuels and biomass. BC particles emitted from these sources are generally hydrophobic, but they are gradually coated by hygroscopic species during transport and become hydrophilic particles with higher cloud condensation nuclei (CCN) activity, and they are finally removed from the atmosphere through wet removal processes. Therefore, wet deposition of BC is one of the most important processes controlling BC concentrations and their distribution. In order to understand the importance of wet removal processes of BC, BC mass concentrations both in the surface air (m_{air}) and in rainwater (m_{rain}) were measured simultaneously for two years (April 2010 - March 2012) at Cape Hedo in Okinawa. This study is the first attempt to conduct long-term measurements of m_{air} and m_{rain} at a remote site in East Asia. Seasonal variations of both concentrations and the wet deposition flux of BC are presented.

A Continuous Soot Monitoring System (COSMOS) was used to measure m_{air} . Rainwater samples were collected on a daily basis and m_{rain} was measured by an ultrasonic nebulizer (U-5000AT) and a Single Particle Soot Photometer (SP2).

The measured m_{air} and m_{rain} showed clear seasonal variations. The monthly mean m_{air} and m_{rain} were the highest during spring (March - May) with the values of 0.37 ug m^{-3} and 62.2 ug L^{-1} , and the lowest during summer (June - August) with the values of 0.07 ug m^{-3} and 5.82 ug L^{-1} . The correlation coefficient between the monthly mean m_{air} and m_{rain} was sufficiently high ($r^2 = 0.67$). The annual average amount of BC wet deposition, which was defined as the product of m_{rain} and precipitation amount, was 39.6 mg m^{-2} during the observation periods. The contribution to the total amounts of BC wet deposition was found to be 74.4% during spring. This is due to both higher m_{rain} and larger precipitation amount in spring. The values of m_{air} and m_{rain} in winter (December - February) and spring are the highest because polluted air masses are frequently transported from the Asian continent by strong north-westerly wind, East Asian monsoon in winter and cold front passages in spring. On the other hand, these values are the lowest in summer because clean air masses are transported from south to the measurement site by the Pacific high.

Keywords: Black Carbon, wet deposition

Number-size distribution of maritime aerosol particles over the Pacific Ocean

Sayako Ueda^{1*}, Kazuhiko Miura¹, Ryou Kawata², Hiroshi Furutani², Mitsuo Uematsu²

¹Tokyo University of Science, ²AORI, University of Tokyo

Size and number concentration of atmospheric aerosol particles are the most fundamental parameters for estimating effects of aerosol on climate. Number-size distributions of aerosol in 10-500 nm diameters were observed on board the R/V Hakuho-Maru cruises over the Pacific Ocean during December 2011-March 2012. The KH-11-10 cruise started from Tokyo and reached Peru via Hawaii and the mid-latitudes eastern South Pacific Ocean. The KH-12-1 cruise started from Peru and reached Tokyo via the eastern equator and Hawaii. Number-size distribution of dried aerosol particles was measured using a Scanning Mobility Particle Sizer (3034, TSI Inc.) for diameters of 10-500 nm and a laser particle counter (LPC, KC01D; RION Co. Ltd.) for diameters greater than 300 nm. The obtained number-size distributions were analyzed to reveal their relationship with the condensation sink of precursor gases, air mass transport, meteorological condition, and chlorophyll concentration along trajectory.

Bimodal size distribution with mode peaks in 30-80 nm (Aitken mode) and 100-200 nm (accumulation mode) was frequently observed. Relatively large mode sizes were observed over the western equator. The 5 days backward trajectory shows that the air masses in equator are originated from the high chlorophyll area without experiencing precipitation. Over the mid-latitudes in the eastern South Pacific where chlorophyll concentration is low, new particle formation event was often observed in accordance with the low concentration of accumulation mode particles.

In this observation, new particle formation event was not observed under high chlorophyll condition over the equator. Condensation of precursor gases onto pre-existing particles strongly prevents nucleation of fresh particles. Because such condensation to pre-existing particles was effective enough in the equator under non-precipitating condition, new particle formation could not be observed over the equator. These results suggested that precipitation and biological productivity controlled the balances of formation and growth of aerosol particles, characterizing the number size distribution over each ocean areas.

Keywords: Maritime aerosol, Number-size distribution, New particle formation

Atmospheric pollutants originated Asian Continent included PM in Yakushima Island.

Osamu Nagafuchi^{1*}, Kuriko Yokota², Kenshi Tezuka³, Mayumi Jige⁴, Koyomi Nakazawa⁵

¹The University of Shiga Prefecture, ²Toyohashi University of Technology, ³Yattane goyou team, ⁴Ootani University, ⁵Osaka University

Airborne particulate matter (PM) is a complex mixture of particles that are very different in size, chemical composition, physical state and morphology. Moreover, PM has a variety of emission sources which range from natural to anthropogenic and stationary to mobile. It also has a variety of physical and chemical properties. Therefore, not only the size distribution of particles but also information related to their chemical composition will play an important role in elucidation of the behavior and major emission sources of PM and their effect on human health and the ecosystem.

The samples of size-resolved PM were collected using a 3-stage NLAS impactor (Tokyo Dyrec Co., Ltd., particle cut size of stage is 10mm, 2.5 mm and 1.0mm for a flow rate of 3 L/min) with one day or three days sampling interval on the poly-carbonate filter (25mmf) and a polycarbonate filter (back-up filter 47mmf). Sampling of the PM was conducted at Yakushima Island, from 13 to 26 Jan., 2013. Elemental compositions of these samples were determined by ICP/MS, and ionic species were analyzed by IC. In addition, we observed a morphology by SEM. Moreover ATR-FT-IR imaging measurements of individual particles were performed using a Perkin-Elmer Spectrum 100 FT-IR spectrometer interfaced to a Spectrum Spotlight 400 FT-IR microscope.

Keywords: particulate matter, long-range transport, major ion, heavy metal

Atmospheric Fe-containing particles over the North Pacific Ocean : the mixing states with water-soluble materials

Yusuke Miki^{1*}, Sayako Ueda¹, Kazuhiko Miura¹, Hiroshi Furutani², Mitsuo Uematsu²

¹Tokyo University of Science, ²University of Tokyo

Fe is an essential element for marine phytoplankton growth. Long-range transportation of atmospheric aerosols from the continent and subsequent deposition is an important process to supply Fe to the ocean. The dry and wet depositions of aerosol particles depend on the particle size and the mixing states with water-soluble materials. In order to study the mixing states of Fe-containing particles with water-soluble materials, we collected aerosol particles on the ship over the mid-latitude western North Pacific Ocean during the KH-12-1 (EqPOS) Leg 2 cruise of the R/V Hakuho Maru, Atmosphere and Ocean Research Institute (AORI), University of Tokyo. The leg started from Hawaii on February 21, 2012, and arrived at Tokyo on March 7, 2012. We collected aerosol particles with a low pressure impactor. Collected particles were analyzed using a transmission electron microscopy (TEM) with a water dialysis method. Most of maritime aerosols are consisted of water-soluble materials such as sea-salt and sulfate particles. Water-insoluble materials such as minerals and industrial metals are main sources of Fe. This study focused on water-insoluble materials and performed an energy-dispersive X-ray (EDX) analysis.

We classified the origins of encountered air masses on the basis of backward air trajectory analysis and number concentration of aerosols measured by an optical particle counter (OPC). Particles larger than $D = 0.5 \mu\text{m}$ during dust events and background conditions (maritime or continental origins) were analyzed using the TEM. Number fractions of particles containing water-insoluble materials were 5-20% (0.5-1.0 μm in diameter) and 15-50% ($>1.0 \mu\text{m}$ in diameter). Most of water-insoluble materials were mixed with water-soluble materials (mixed particles). Median values of the volume percent of the water-soluble materials in the mixed particles on a maritime sample were $>90\%$ and those on the other samples were 60-80%. Based on EDX analyses of water-insoluble materials, number fractions of Fe-containing particles were 2% (maritime), 2% (continental) and 8% (dust event), respectively. Fe-containing water-insoluble materials were found with other mineral components (Si or Al), and mixed with water-soluble materials.

Since phytoplankton growth requires dissolved form of Fe, we performed EDX analyses for the same particles before and after extractions of water-soluble materials from particles to estimate fraction of water-soluble Fe. The amount of Fe after the extraction was smaller comparing with the amount of Fe before the extraction, indicating that the water-soluble Fe is presented with the water-insoluble Fe.

Keywords: Fe, water-soluble materials, water-insoluble materials, dust, aerosol

Evaluation of the method to measure black carbon particles suspended in rainwater and snow samples

Sho Ohata^{1*}, MOTEKI, Nobuhiro¹, SCHWARZ, Joshua P.², FAHEY, David W.², Yutaka Kondo¹

¹Department of Earth and Planetary Science, Graduate School of Science, The University of Tokyo, ²Earth System Research Laboratory, National Oceanic and Atmospheric Administration

The mass concentrations and size distributions of black carbon (BC) particles in rainwater and snow are important parameters for improved understanding of the wet deposition of BC. In this study, we have made a detailed evaluation of the method to measure these parameters. The method consists of an ultrasonic nebulizer (USN) and a Single Particle Soot Photometer (SP2). The USN converts sample water into micron-size droplets at a constant rate and then extracts BC particles to air by drying the water droplets. The mass of individual BC particles is measured by the SP2, based on the laser-induced incandescence technique. The loss of BC particles during the extraction process from liquid water to air depends on their sizes. We determined the size-dependent extraction efficiency using polystyrene latex spheres (PSLs) with twelve different diameters between 107-1025 nm. The PSL concentrations in water were measured by the light extinction at 532 nm. The extraction efficiency of the USN showed broad maximum of about 10% in the diameter range of 200-500 nm, and decreased substantially at larger sizes. Total uncertainty and reproducibility of the measured mass concentration of BC in sample water were $\pm 40\%$ and $\pm 35\%$, respectively. Measured BC size distributions in rainwater and surface snow collected in Tokyo, Okinawa, and Sapporo showed negligible contribution of the BC particles larger than 600 nm to the total BC amounts. However, surface snow collected in Greenland sometimes contained significant amount of larger BC particles, beyond the upper detection limit of the present method.

Keywords: black carbon, wet deposition

Emission of biogenic VOCs from evergreen broadleaf tree: variation in composition of monoterpenes

Sou Matsunaga^{1*}, TAKAGI, Masahiro², KUSUMOTO, Dai³, HIURA, Tsutomu¹

¹Tomakomai Research Station, Hokkaido University, ²Faculty of Agriculture, University of Miyazaki, ³The University of Tokyo Tanashi Forest, the University of Tokyo

Introduction

Biogenic volatile organic compound (biogenic VOC, BVOC) is known to have an important role on atmospheric chemistry in both regional and a global scale. BVOCs consist of many classes of organic compounds such as isoprene (C_5H_8), monoterpenes (MNTs: $C_{10}H_{16}$) and others. Although emission pattern of isoprene, which has the largest emission rate, is relatively well modeled as a result of many efforts, that of monoterpene is still uncertain and seems to be much more complicated compared to isoprene. There should be a consistent reason for plants to synthesize and emit BVOCs because the emission of BVOCs requires considerable cost. However, there has not been any unified understanding on the factor controls BVOC emission, yet. To solve this mystery, emission of MNTs under "natural" environment should be one of the hopeful objects because MNTs are known to have variable effect to survive in the environment (e.g. avoidance of herbivory) and because MNTs consist of numerous isomers, it implies the MNT emissions may contain higher information than other single BVOC such as isoprene. MNTs are, in general, known to be emitted from coniferous trees. Some of evergreen broadleaf (EB) trees also emit MNTs. However, report about MNT emission from the EB tree is still quite limited. Only a few EB species emit the BVOCs while other EB species emits no BVOCs even they live in the same community. Although they are living in similar environmental condition, BVOC emission of the EB trees quite differ each other. We hypothesized that there might be a clue to reveal the fundamental principle which determines and controls the BVOC emission. In this presentation, we report a preliminary result of BVOC measurement targeted on the dominant EB trees in Japan.

Experiment

Screening samples were collected for seven EB tree species using a blanch enclosure at the university of Tokyo Tanashi Forest in July 2012. The intensive sample collection has been conducted in Tano Forest Science Station of Miyazaki University ($31^{\circ}51'8''N$ $131^{\circ}18'23''E$) from 25th through 28th September 2012. The BVOC samples were collected from twenty *Castanopsis sieboldii* leaves into a glass tube filled with adsorbents using a leaf cuvette on the top of 15 m canopy tower in EB tree community. The samples were analyzed employing a gas chromatograph (GC-FID) coupled with a cryo-focus and thermal desorption system.

Result and discussion

As a result of the screening, only *Castanopsis sieboldii* was found to be MNT emitter among investigated EB trees. The MNT emission rates ranged from 0.04 - 30 (alpha-pinene) $\mu g C g^{-1} h^{-1}$. The averaged total MNT emission rate was 19 $\mu g C g^{-1} h^{-1}$, it is comparable to or exceeds that of *Pinus* trees which is commonly known as major MNT emitter. Light dependence on the emission was not clearly observed. The emission rates were normalized to obtain basal emission rate, which can be regarded as "emission activity", based on G93 temperature dependence model with empirical coefficient *beta* of 0.10. Figure 1 shows composition of MNT basal emission rates. A clear contrast of the composition among the individuals can be observed while total emission rates were relatively close each other. Individual 1 emitted sabinene as the most abundant MNT while ocimene was one of minor MNTs. On the contrast, individual 2 and 3 emitted ocimene as 2nd or 3rd most abundant MNT while sabinene was minor MNT. Although these individuals are same tree species and are almost same ages, in addition, growing in quite similar environment (within only 1-2 m of distance each other), the composition of the MNTs showed a clear difference. It can be hypothesized that the *C. sieboldii* trees emitted different types of MNTs as responses to stresses they are exposed to. In other words, spatial distribution of BVOC emitting / non-emitting trees and/or the distribution of BVOC types in the community probably contain a clue to the mystery of fundamental factor of the BVOC emissions.

Keywords: Biogenic Volatile Organic Compound, Atmospheric Chemistry, Biosphere Atmosphere Interaction, Biogeoscience, Material Cycle, Evergreen Broadleaf Tree

AAS21-P17

Room:Convention Hall

Time:May 19 18:15-19:30

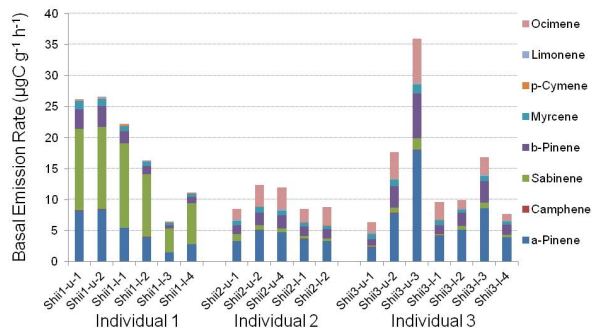


Figure 1 Basal emission rates of monoterpenes emitted from *Castanopsis sieboldii* trees obtained by leaf level BVOC measurement.

Comparison of concentrations and photoreactivities of oxalic acid and metal-oxalate complexes in aerosols

Yoshiaki Yamakawa^{1*}, Kohei Sakata², Aya Sakaguchi², Yoshio Takahashi²

¹Faculty of Science, Hiroshima University, ²Graduate School of Science, Hiroshima University

Aerosols have cooling effect to the earth, which is divided into direct and indirect effects. The direct effect is reflection of sunlight directly by aerosols, whereas the indirect effect is the reflection by clouds formed by the aid of aerosols working as cloud condensation nuclei (CCN). Oxalic acid is a main component of secondary organic aerosols (SOA) and abundant in the atmosphere, which is formed by degradation of organic components with longer carbon chain such as malonic acid. Oxalic acid is hygroscopic, which works as CCN with indirect cooling effect. It has been estimated that the degree of cooling effect by the aerosols are equal to that of the warming effect of carbon dioxide. However, there is large uncertainty in the estimation. In fact, if oxalic acid forms insoluble metal-oxalate complexes in the atmosphere, it is possible that the indirect effect can be smaller than the estimation. In addition, in the presence of metal-complex, it is also important to understand the formation processes. Therefore, this study was aimed (i) to decide the ratio of insoluble metal-oxalate complexes to oxalic acid in the aerosols by X-ray absorption fine structure (XAFS) spectroscopy to contribute to precise prediction of global warming and (ii) to evaluate stabilities of oxalic acid and metal-oxalate complex in the atmosphere during the photoreactions. The latter factor can be related to the dominance of metal-oxalate complexes in the atmosphere, if we can show that the photodegradation reactivity of oxalic acid is much larger than that of metal-oxalate complex by ultraviolet light.

We collected size-fractionated aerosols at Higashi-Hiroshima to determine chemical species of oxalic acid. As a result, (i) zinc (Zn) oxalate complex was found in fine particles (< 2.1 micron) and (ii) calcium (Ca) complex was present in all the particle sizes except for the 4.2 to 10.2 micron particles. Oxalic acid is SOA that is formed by degradation of organic matters, whereas oxalic acid can be distributed to the particle size from 0.5 to 1.0 micron known as droplet mode, where metal-oxalate complexes can be formed.

To estimate the stabilities of oxalic acid and its metal-oxalate complex with Mg^{2+} , their photodegradations by ultraviolet lights in water were determined by measuring their concentrations at various elapsed time using total organic carbon analyzer. As a result, there was no appreciable difference between the two systems up to 8 hours, but the concentration of the complex was kept larger than that of oxalic acid after 8 hours. Therefore, it is possible that oxalic acid actually exists as metal-oxalate complex in the atmosphere possibly by preferential photodegradation of oxalic acid.

We will also analyze chemical species employing XAFS analysis on other metal ions such as lead and copper to measure precisely the ratio of metal-oxalate complex to total oxalate species. We will also conduct photodegradation experiments by ultraviolet light not only for Mg^{2+} complex but also for Zn^{2+} and Ca^{2+} complexes to confirm the difference of photodegradation caused by chemical species.

Keywords: aerosol, metal-oxalate complex, indirect cooling effect, photoreactivity, X-ray absorption fine structure

Vertical profiles of aerosol size distributions near the surface boundary layer

Masanori Yabuki^{1*}, Kenshi Takahashi¹, Makoto Matsuda¹, Toshitaka Tsuda¹

¹Research Institute for Sustainable Humanosphere, Kyoto University

Knowledge of the properties of the atmospheric minor constituents is essential in studies on climate change and its effects on human health. The concentrations of ambient trace gases and aerosols, which are emitted by both natural and anthropogenic sources, are influenced by diffusion due to the thermodynamic processes during the air-mass transportation along the prevailing wind flow. Their chemical and physical properties vary both temporally and spatially as a result of various atmospheric processes such as scavenging, nucleation, evaporation, and condensation. Therefore, a comprehensive approach that takes into consideration atmospheric chemistry as well as dynamics and thermodynamics is required for a thorough understanding of air quality.

For elucidating the properties of the minor constituents in the surface boundary layer, we have carried out AEROSol and GASes Profiling (AEROGAP) experiments using a combination of in situ and remote sensing measurements at the Kyoto University Middle and Upper Radar site (34.9 N, 136.1 E) in Shiga Prefecture, Japan, during the summers of 2011 and 2012. In this study, we focus on the temporal variations in the vertical profile of nano- and submicron particles observed by a condensation particle counter and an optical particle counter fixed to tethered balloon platforms. We also discuss the properties derived from aerosol lidar observations compared with those observed using in situ instruments.

Keywords: Aerosol, Size distribution, Tethered balloon, Lidar

Measurement of organic nitrates in the atmosphere using thermal dissociation/cavity attenuated phase shift spectroscopy

Yasuhiro Sadanaga^{1*}, Ryo Takaji¹, Kazuo Nakajima¹, Kazunari Suzuki¹, Atsushi Matsuki², Keiichi Sato³, Hiroshi Bandow¹

¹Osaka Prefecture University, ²Kanazawa University, ³Asia Center for Air Pollution Research

Peroxyacyl nitrates (PANs) and alkyl nitrates (ANs) act as one of the reservoirs of nitrogen oxides (NO_x) in the atmosphere. Since their lifetime is longer than that of NO_x , they can be transported over a long-distance and would be important as trans-boundary pollutants. PANs and ANs are generally observed using GC/ECD (gas chromatograph / electron capture detector) or GC/NICI-MS (gas chromatograph / negative ion chemical ionization-mass spectrometry) method. While these GC methods can measure concentrations of each constituent in PANs and ANs, they have low time resolution. Measurements by GC/ECD which has radioisotope are very difficult in Japan because of laws and regulations. On the other hand, frequent maintenances are required for measurements using GC/NICI-MS. Thus observation data of PANs and ANs in Japan are quite low.

In this research, continuous measurement system of total PANs and ANs in the troposphere has been developed by using a thermal dissociation / cavity attenuated phase shift spectroscopy (TD/CAPS) method. Both PANs and ANs are thermally decomposed to produce NO_2 and then NO_2 is measured by CAPS method. This system can observe PANs and ANs with high time resolution while this system cannot separate constituents of PANs and ANs.

This system has three lines; (1) NO_2 line, (2) PANs line, and (3) ANs line. The NO_2 line consists of a quartz tube without heating. The PANs and ANs lines have quartz tubes heated at 433 K and 633 K, respectively. Concentrations of NO_2 , NO_2 + PANs and NO_2 + PANs + ANs can be obtained from the NO_2 , PANs and ANs lines, respectively. These concentrations are sequentially measured by switching solenoid valves and then NO_2 , PANs and ANs concentrations are obtained. Since a part of HNO_3 is pyrolyzed in the ANs line, annular denuder coated with NaCl to remove HNO_3 is set before the heated quartz tube in the ANs line.

The decomposition efficiencies of PANs and ANs were investigated and obtained to be 100 and 90%, respectively, for all kinds of PANs and ANs examined.

Continuous field observations of PANs and ANs concentrations have been being carried out at NOTOGRO supersite at Suzu, Noto Peninsula, since November 2012. In this presentation, the observational results and preliminary analyses of PANs and ANs concentration variations with NO_x , NO_y , total inorganic nitrate, O_3 and CO concentrations simultaneously observed are introduced.

Keywords: total odd nitrogen species, organic nitrates, cavity attenuated phase shift spectroscopy

Chemical composition of the SCPs derived from fossil-fuel combustion in East Asia and their long transportation

INOUE, Jun^{1*}, MOMOSE, Azusa¹, OKUDAIRA, Takamoto¹, KITASE, Akiko M.², YAMAZAKI, Hideo³, KAMURA, Kazuo², YOSHIKAWA, Shusaku¹

¹Osaka City University, ²Waseda University, ³Kindai University

Spheroidal carbonaceous particles (SCPs) are produced by the high-temperature combustion of fossil fuels (e.g., in thermal power station) and are emitted to the atmosphere. They are unambiguous indicators of atmospheric deposition from industrial fossil fuel combustion. We examined elemental composition of the particles in surface sediments nearby industrial cities in East Asia to clarify the elemental characteristic of the particles emitted from each country. Then we also analysed the particles in surface sediments collected in islands in Sea of Japan and the sites along the sea to clarify their source area. We collected 9 samples in Japan, 6 samples in China, 6 samples in Korea, and 5 samples in Taiwan as samples of industrial cities, and 4 samples in remote islands in Japan Sea, and 3 samples at sites along the sea as samples of remote area. We used EDS (energy dispersive spectroscopy) to quantitatively analyze the concentrations of Na, Mg, Al, Si, P, S, Cl, K, Ca, Ti, V, Cr, Mn, Fe, Co, Ni, Cu, and Zn in the particles. As a results, the compositions of SCPs differ among Japanese, Chinese, Korean and Taiwanese cities, especially in terms of Si, S and Ti; particles in Japan and Korea are enriched in Si and S, particles in China are enriched in Si and Ti, and particles in Taiwan are enriched in Si, S and Ti. Results of liner discriminant analysis indicate the particles in each country are discriminated with high reliability of approximately 90%, based on their chemical composition. Based on these discriminant functions, the particles in Oki Islands, Iki Islands and Goto Islands were classified to three types of Japan-Korea type, China Type and Taiwan type. Over 30% of china type was recognized in each sample in these Islands, that are probably derived from China.

Keywords: spheroidal carbonaceous particles, fossil-fuel combustion, chemical composition, East Asia, long transportation

Simulation of aerosol-cloud interactions in spring over East Asia using WRF-chem model : Comparison with aircraft obs.

Ray Takatani^{1*}, Makoto Koike¹, Hitoshi MATSUI¹

¹University of Tokyo

1. Introduction

Aerosols act as cloud condensation nuclei and increase/decrease cloud droplet number concentrations. They play an important role for cloud microphysics, dynamics, and radiative forcing. Recently, various observational and modeling studies have been conducted to understand aerosol-cloud interactions in the lower stratus over the Eastern Pacific (e.g., California, Chile) However, there are still few studies focused on aerosol-cloud interactions over East Asia, although aerosol concentrations are considerably high and large aerosol-cloud interactions are expected over the regions.

In this study, we calculated aerosol and cloud droplet number concentrations using a regional three-dimensional model, WRF-Chem, which explicitly expresses the impact of aerosols on cloud microphysics processes. The purpose of this study is to validate model-calculated aerosol and cloud droplet concentrations with the observation during the A-FORCE aircraft campaign.

2. A-FORCE aircraft observation

Our target is low-level stratus/stratocumulus clouds (< 2km in altitude) without precipitation. During the A-FORCE campaign, aerosol number concentrations below the cloud base and cloud droplet number concentrations just above the cloud base were observed 9 times over the Yellow Sea and the East China Sea in March and April 2009 [Koike et al., 2012].

3. WRF-Chem model calculation

Model simulations were conducted over East Asia using the WRF-Chem v3.4. The simulation periods are from 21 March to 26 April 2009. We used 3 domains with the horizontal grid resolutions of 108km, 36km, and 12km, respectively. Vertical resolutions are 46 layers from the surface to 100 hPa (the lowest layer is about 30m). Both anthropogenic and biomass burning emissions are considered in the simulation. Chemical and microphysical processes of aerosols were calculated by the MOSAIC module with 8 size bins. The Morrison double moment scheme was used for cloud microphysics.

4. Results

Mean observed and calculated aerosol number concentrations (>130 nm in diameter) have good agreement within 30% (underestimation by 27% by model). They also have a positive correlation ($r^2=0.32$), suggesting that spatial and temporal variations of aerosol number concentrations (the transport of anthropogenic aerosols from the Asian continent) were generally reproduced by the model. On the other hand, cloud droplet number concentrations were overestimated by 90%, while a good correlation ($r^2=0.83$) was found between measurements and model simulations.

To quantify the impact of aerosols on cloud microphysics, we compared the relationship between aerosol (>130nm in diameter) and cloud droplet number concentrations. Positive correlations are found for both measurements and simulations. However, the ratio of cloud/aerosol number concentrations is by overestimated by 170% by the model. The potential reasons of this overestimation are 1) the underestimation of entrainment and 2) the overestimation of aerosol activation to cloud droplets in the model.

Keywords: aerosol, cloud, indirect effect, numerical simulation

Model inter-comparison for evaluation on source sensitivities of atmospheric pollutants over East Asia

Kazuyo Yamaji^{1*}, Kohei Ikeda¹, Masayuki Takigawa¹, Tatsuya Nagashima², Yugo Kanaya¹

¹Japan Agency for Marine-Earth Science and Technology, ²National Institute for Environmental Studies

Atmospheric pollutants were simulated by using two regional CTMs, WRF-Chem and WRF/CMAQ and a global CTM, CHASER over East Asia for the year 2005. Simulated surface O₃ over Japan by WRF/CMAQ was higher than that by CHASER especially in summer, and overestimated observed O₃ at EANET monitoring sites. Contributions from 5 source regions; north China(CHN), central China(CHC), and south China(CHS), Korea(KRE), and Japan(JPN) on 6 areas on these regions were evaluated based on sensitivity simulations with 20% reduction in anthropogenic emissions. These models resulted that the 20% emission reductions on CHC would gain 0.8% decrease of surface O₃ over Central Japan in spring, and that was comparable to the O₃ decrease of 0.8-0.9% over Central Japan by the 20% emission reductions on JPN. As for the summer case by using CHASER, the O₃ decreases of 0.6% and 1.6% over Central Japan by 20% emission reductions over CHC and JPN, respectively. On the other hand, the regional CTMs, WRF-Chem and WRF/CMAQ, resulted 0.9% (CHC emission reduction) and 3.1% (JPN) O₃ decreases and 0.7%(CHC) and 2.4% (JPN) O₃ decreases, respectively, and that were 1.2-1.9 times higher than those by CHASER.

Keywords: air quality models, East Asia, atmospheric pollutants, ozone, PM_{2.5}, inter-comparison

Dynamics of particulate matter in the atmosphere

keisuke ikeda^{1*}, Osamu Nagafuchi¹, Ken'ichi Osaka¹

¹Graduate School of Environmental Science, the University of Shiga Prefecture

In recent years, due to the rapid economic growth and industrial development, many air pollutants from East Asian regions are discharged into the atmosphere. This trend is seen to continue, transboundary pollution to Japan may become more serious. In this study, we collected particulate matter at two points. One is the surface layer which we live, and the other is the atmospheric boundary layer whose air is easily transported. Our purpose is the elucidation of particulate matter dynamics and of the effect of transboundary pollution from East Asia.

Collecting particulate matter is conducted on period between April, 11, 2012 and August, 3, 2012 at the University of Shiga Prefecture as the surface layer and on period between October, 17, 2012 and November 22, 2012 at the Mt. Ibuki in Shiga prefecture as the atmospheric boundary layer. Sample we collect is measured ion component by ion chromatography and heavy metal by ICP-MS. Analysis of backward trajectories used HYSPLIT model provided by NOAA.

At the surface layer, we observed NO_3^- , NH_4^+ , nss SO_4^{2-} , nss Ca^{2+} at high concentrations, when we observed yellow sand in spring. At this time, the air mass comes from the continent. On the other hand, same trend was not seen in summer. At this time, the air mass comes from the ocean. Forms of deposition are mainly NH_4NO_3 , $(\text{NH}_4)_2\text{SO}_4$, $\text{Ca}(\text{NO}_3)_2$, CaSO_4 during observing period.

At the atmospheric boundary layer, we didn't observe same trend as the surface layer. Forms of transport are mainly NaNO_3 , Na_2SO_4 during observing period. This indicates that NaCl which derived from sea salt is altered by HNO_3 and SO_2 .

Keywords: particulate matter, transboundary pollution, yellow sand

Calculated mercury deposition in north of Lake Biwa

Naoko Hishida^{1*}, NAGAFUCHI, Osamu², OSAKA, Ken'ichi², MIYAKE, Takayuki²

¹Environmental Science Graduate School, the University of Shiga Prefecture, ²the University of Shiga Prefecture

Gaseous elemental mercury (GEM) account for above 95% out of the atmosphere of mercury, have the property that is hard to dissolve in water and circulates through the whole earth with the atmosphere. GEM becomes reactive gaseous mercury (RGM) that is easy to dissolve in water by the oxidation, and it is removed by deposition from the atmosphere with particle-mercury (p-Hg). Therefore mercury concentration in precipitation may elevate at the place apart from the mercury emission source. Furthermore, mercury removed from all over the atmosphere by deposition is in aquatic area and bioaccumulates in the process of the food chain. In this study, it was intended that calculated mercury deposition from mercury concentration in precipitation in north of Lake Biwa.

Sampling site is Surumi in north of Shiga prefecture there is annual mean precipitation 2800mm and classified in the heavy snowfall area. Two forms samplers, one is automatic rain sampler for researched a change of the mercury concentration in precipitation in one rain, and one is bulk deposit sampler for calculated mercury deposition in here. Automatic rain sampler developed so that every fixed quantity collected precipitation (as for every 5mm). Precipitation sampling was conducted from June to November, 2011 and from March to November, 2012. Sampling was not able to observe it for the snow in the winter season (from December to February). From July, 2012, samples were filtered by PTFE filter, and measured by alkali reduction cold vapor atomic fluorescence spectrometry.

It was 29 rain that samples were collected by September, 2012, and the total mercury concentration in precipitation fluctuated from 1.09 to 25.9 ng/L, and mean was 7.15 ± 5.31 ng/L. Pattern that became least concentration to begin to fall was frequent, but total mercury concentrations change in one rain did not showed constant pattern. By the precipitation with the typhoon of September, 2011, total mercury concentration in precipitation gradually rose. When rain cloud arrived at Surumi through mercury emission areas, mercury concentration rises. It is thought that the change of the mercury concentration in precipitation is related to the passage course of the rain cloud. In addition, mercury deposition that calculated from bulk deposit samples became 19.7 g/km²/year (from September, 2011 to August, 2012).

Keywords: mercury, deposition, Lake Biwa

Atmospheric mercury in the free troposphere

Yuki Nishida^{1*}, Osamu Nagafuchi², Ken'ichi Osaka², Takayuki Miyake²

¹Environmental Science Graduate School, the University of Shiga Prefecture, ²School of Environmental Science, the University of Shiga Prefecture

In order to clarify the dynamics of atmospheric mercury in the free troposphere (FT), continuous observation of atmospheric mercury were carried out in Norikura Solar Observatory in Japan. The observation period is one week each of Oct 2011 and Oct 2012. Gaseous mercury (TGM) and particulate mercury (PHg) concentration in Norikura Oct 2011 were 0.72 - 1.23 ng m⁻³ and 17.0 - 121.0 pg m⁻³, respectively. TGM concentration in 2012 was 0.2 - 2.4 ng m⁻³, and the mean was 1.6 ng m⁻³. A diel variation of TGM was observed with daytime highs and nighttime lows in almost all of both periods. This diel pattern is considered to be due to upslope wind of boundary layer air resulting from a mountain surface that is warmed up with sunlight in daytime. Therefore such observation of atmosphere in the FT to use mountains, data is collect at night. In addition, the observation of 2012, sharp rise in the TGM concentration has been observed. Almost simultaneously with the concentration increasing of TGM, temperature has dropped drastically, and we saw a half inches of snow. This is thought to be due to cold air mass that flowed into Japan came from the continent, this suggested the possibility of long-distance transport of mercury.

Keywords: mercury, atmospheric chemistry, free troposphere, long - range transport

Measurement of fluorescent particles in Fukue Island

Fumikazu Taketani^{1*}, Xiaole Pan¹, Yugo Kanaya¹

¹JAMSTEC

Among various optical techniques applied for the atmospheric particle detection, fluorescence is useful for detecting certain types of organic particles, especially those of biological origin. In this study, we employed a single-particle fluorescence sensor, WIBS-4, for the detection of fluorescent particles, to demonstrate the capability of the classification of organic particles in the ambient air.

We conducted ambient air measurements from Sep 16 to Dec 14, 2011 using the WIBS-4 instrument at Fukue Island (32.75N, 128.68E) in Japan. We detected 36,000,000 particles during the observation period, and the ratio of the fluorescent particles to the total varied in the range of 2 - 65%. In Oct.6, high number concentrations were observed, suggesting transportation from the continent by the trajectory analysis. During this period, the ratio of the fluorescent particles to the total was about 50%, suggesting that transported particles include fluorescent material. In the presentation, we will discuss the comparison of fluorescence pattern from individual particles.

Keywords: aerosol, fluorescence

Inhomogeneity of NO₂ over Fukuoka, an urban site in Japan observed by MAX-DOAS

Hisahiro Takashima^{1*}, Yugo Kanaya², Kodai Ito¹

¹Faculty of Science, Fukuoka University, ²JAMSTEC/RIGC

Since August 2012, continuous NO₂ observations have been performed using ground-based Multi-Axis Differential Optical Absorption Spectroscopy (MAX-DOAS) at Fukuoka (33.55N, 130.36E), an urban site in Japan. MAX-DOAS is a passive remote sensing technique using scattered visible and ultraviolet solar radiation at several elevation angles. We investigate inhomogeneity of NO₂ by observing at two azimuth angles, Tenjin (downtown area) direction and Itoshima (out of downtown area) direction. We discuss the observed inhomogeneity with a focus on the three factors: inhomogeneity of NO₂ emissions, development of the boundary layer, horizontal transport associated with land/sea breeze.

A Study on Detection Methods for Atmospheric Small Particles Based of Lidar Techniques

Yutong Liu^{1*}, Masanori Yabuki¹, Toshitaka Tsuda¹

¹Research Institute for Sustainable Humanosphere

Knowledge of the aerosol size distribution in the accumulation mode (50-1000 nm) is essential in studies on human health because small particles could even penetrate into lung foam, thus increasing the risk of bronchitis or lung and heart diseases. Optical Remote sensing techniques such as a lidar are effective for monitoring aerosols with high temporal and spatial variations. Aerosol instruments using light of wavelengths 350-1500 nm have been put into practical use, and they are effective for detecting particles with sizes comparable to the wavelength. However, to estimate quantitatively the shape of the particle size distribution, more information of small particles with radii around 100nm is required.

In this study, a lidar analysis method is proposed to derive the aerosol size distribution for a wide range of particle sizes, including 100 nm. The algorithm can be divided into two parts. The first part applies the conventional analysis using the wavelength dependence of aerosol physical parameters based on single scattering lidar techniques. The second part involves the use of multiple scattering via multiple-filed-of-view lidar signals for achieving a probing wavelength less than 350 nm; although such short wavelengths can be used to obtain information on small particles, they have not been used for aerosol measurement owing to the strong light absorption by atmospheric constituents such as ozone. The analysis is accomplished by directly fitting the observed lidar signals and the retrieved aerosol parameters to the theoretical values that are based on the look-up-table which is constructed on the basis of Mie scattering and multiple scattering calculations as a function of the log-normal size distribution.

The retrieved particle mode radii in a range of 50-200 nm agree with the originally assumed parameters in combination of single scattering and multiple scattering algorithms, even if noise is contained. In order to evaluate the noise effect, we simulated a sensitivity analysis. When random errors of 5%, 10%, 20%, and 50% were added to the prepared parameters theoretically calculated by use of the geometric mean radius of 100 nm for the aerosol size distribution, the retrieved mean radius (upper and lower limits) derived from the proposed method were 103 nm (83-128 nm), 100 nm (69-144 nm), 89 nm (48-163 nm), and 84 nm (38-186 nm), respectively.

Keywords: Lidar, Aerosol

Development of a scanning Raman lidar for observing the spatio-temporal distribution of water vapor

Makoto Matsuda¹, Masanori Yabuki^{1*}, Toshitaka Tsuda¹, Kenshi Takahashi¹, Ken-ichi Yoshikawa¹

¹Research Institute for Sustainable Humanosphere, Kyoto University

Water vapor and aerosol particles are important atmospheric constituents that play a key role in the atmospheric processes such as thermodynamics, radiative forcing, cloud physics, and chemistry. Atmospheric constituents near the surface are highly variable spatially and temporally, because of the complex turbulent flow over the surface. It is required to innovative techniques for observing the distributions of atmospheric constituents with good spatio-temporal resolution. We have newly developed a scanning Raman lidar to measure the spatio-temporal distributions of the water vapor and aerosol particles near the surface, which is useful to study the detailed behavior of meteorological phenomena as well as interactions of aerosol particles with water vapor.

Considering the eye-safe operation in urban districts, we employed the UV laser of 355 nm. We developed a scanning mirror system which comprises with highly reflective mirrors and a rotational stage. By use of the program-controlled rotational stage, vertical scan into any zenith direction can be operated with a maximum speed of 1.8 deg./s. Differences between the temporal variations of water vapor mixing ratio by the scanning Raman lidar and those by the conventional lidar for observing a vertical point are less than 2.5 %. It is indicated that the developed system can measure water vapor correctly though the scanning system is attached.

We have demonstrated the potential of the scanning Raman lidar in the forest region at the Shigaraki MU observatory in August and October, 2012. We performed a vertical scan in a zenith sector of 48 deg. with a constant step width of 1.5 deg. The temporal resolution of each pointing direction was 30 s. In this observation, we found that water vapor mixing ratio within the surface boundary layer varied in a range of 13.5 - 16.5 g/kg within the range of 400 m. It is suggested that the spatial variations are highly sensitive under the different topography. During the vertical plane measurements with the wide range scanning, it is found that the thickness of the atmospheric boundary layer changes into the range of about 200m according to the observed directions. During the high spatial and temporal resolution measurements with the continuous scanning at a constant speed, a single cross-sectional distribution can be acquired every 90 s; this indicates the possibility of understanding the cloud formation and modification processes via continuous observations. Scanning Raman lidar has an advantage of obtaining a detailed structure that is difficult to gather from other instruments.

Keywords: lidar, water vapor, aerosol

Parametric studies on temperature lidar with a multispectral detector

Kenichi Yoshikawa^{1*}, Masanori Yabuki¹, Toshitaka Tsuda¹

¹Research Institute for Sustainable Humanosphere, Kyoto University

Measurements of atmospheric temperature and water vapor in the troposphere are essential for studying atmospheric processes such as dynamics, thermodynamics, and cloud physics. Remote sensing techniques have obvious advantages for continuous observation of the spatial distributions of meteorological parameters. The Raman lidar is a laser-based remote sensing instrument used to quantify the distribution of water vapor mixing ratio and atmospheric temperature. We have developed several Raman lidar systems that measure water vapor by detecting the vibrational Raman scattering. Recent improvements in the performance of optical components have led to the development of better water vapor lidar systems that are portable and easy to use. More detailed spatio-temporal distributions of water vapor can be acquired by a lidar equipped with a scanning mirror system. On the other hand, the polychromator design for temperature lidar is much more complex than that for water vapor, because the temperature lidar method is based on the fact that the intensities of the lines within the rotational Raman band exhibit slightly different dependencies on temperature. Therefore, temperature lidar is used less widely than the water vapor system.

In this study, temperature lidar with a multispectral detector is proposed to construct a system that is compact, robust, and easy to align for the detection of rotational Raman signals. The multispectral detector enables 32-channel simultaneous photon counting acquisition and provides spectral and range-resolved data by applying lidar techniques. While conventional temperature lidar methods detect the ratio of two rotational Raman lidar signals of opposite temperature dependence in combination with several edge and interference filters, the multispectral lidar detector can grasp the shape of the rotational Raman spectrum. Therefore, the estimation of temperature can be accomplished by directly fitting the observed lidar signals to the shape of the theoretical values of a rotational Raman spectra that exhibit different dependencies on temperature. The use of the multispectral detector for detecting rotational Raman signals has several advantages. In particular, it can reduce uncertainties in the optical alignment of the polychromator and in the stability of the laser wavelength. Furthermore, the multispectral receiver system can be made more compact and less expensive than the conventional system with an interference-filter-based polychromator.

The accuracy of temperature derived from multispectral lidar signals depends on both the spectral resolution and spectral range of the multispectral detector. Therefore, the values of these parameters should be set appropriately to improve the accuracy of temperature estimation. In this study, we estimated the effect of both spectral resolution and spectral range on the accuracy of temperature estimation, and found the ideal combination of those optical parameters. Then, we calculated the accuracy of our proposed method for temperature estimation via a computer simulation of selected cases in combination with both the spectral resolution and spectral range of a multispectral detector.

Keywords: temperature lidar, multispectral detector

NMD Fractionation Estimated from SO Isotopologues Photolysis UV Spectra

Sebastian Danielache^{1*}, Tomoya Suzuki¹, Shinkoh NANBU¹, Yuichiro Ueno¹

¹Department of Materials & Life Sciences, Faculty of Science & Technology, Sophia University, ²Department of Earth and Planetary Sciences, Tokyo Institute of Technology

Understanding the mechanism of sulfur isotopic fractionation phenomena has been used for some time as a tool to the understanding of reducing atmospheres. Sulfur Non-Mass Dependent (NMD) fractionation signals reported for the Archean and Early Proterozoic (>2300 Ma) atmosphere where the photodissociation of sulfur bearing species play a significant role since the concentration of oxygen is estimated to be 10⁻⁵ times present atmospheric levels and therefore ultraviolet light permeates throughout the entire atmosphere, however the underlying mechanisms are not fully understood. In order to explain the NMD signal preserved in the geological record other than SO₂ photodissociation chemistry of sulfur compound should be taken into account. In this study we consider isotopic fractionation during photodissociation of SO. Experimental studies are difficult since SO is highly reactive and unstable under most experimental and atmospheric conditions. Consequently, theoretical studies are suitable to evaluate its spectroscopic properties. We report ultraviolet absorption cross sections for ^{32,33,34,36}SO isotopologues. R-matrix theory was employed to compute absorption cross sections. Potential energy curves were calculated at multi-reference correlation interaction (MRCI) method with augmented correlation consistent polarized valence sextuple-z (aug-cc-pV6Z) basis set. The six lower-lying electronic states were explored. Because there are pseudo-crossings between electronic excited states, non-adiabatic effect has been taken into account. Isotopic fractionation constants were theoretically estimated at difference temperatures by assuming that the photolysis rates are proportional to the photoabsorption cross sections for each isotopologues. We make the one box model of the atmospheric chemistry where obtained photolysis rates are utilized, and discuss the results of this model.

Keywords: Sulfur Cycle, Archean Atmosphere, Stable Isotopes